



UNIVERSITÀ DI PARMA

ARCHIVIO DELLA RICERCA

University of Parma Research Repository

Investigation of the salicylaldehyde thiosemicarbazone scaffold for inhibition of influenza virus PA endonuclease

This is a pre print version of the following article:

Original

Investigation of the salicylaldehyde thiosemicarbazone scaffold for inhibition of influenza virus PA endonuclease / Rogolino, Dominga; Bacchi, Alessia; De Luca, Laura; Rispoli, Gabriele; Sechi, Mario; Stevaert, Annelies; Naesens, Lieve; Carcelli, Mauro. - In: JBIC. - ISSN 0949-8257. - 20:7(2015), pp. 1109-1121. [10.1007/s00775-015-1292-0]

Availability:

This version is available at: 11381/2810158 since: 2021-09-30T12:35:31Z

Publisher:

Springer Verlag

Published

DOI:10.1007/s00775-015-1292-0

Terms of use:

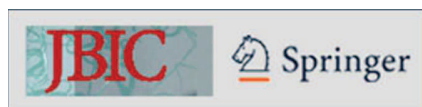
Anyone can freely access the full text of works made available as "Open Access". Works made available

Publisher copyright

note finali coverpage

(Article begins on next page)

24 July 2024



Investigation of the Salicylaldehyde Thiosemicarbazone Scaffold for Inhibition of Influenza Virus PA Endonuclease

Journal:	<i>Journal of Biological Inorganic Chemistry</i>
Manuscript ID:	Draft
Manuscript Type:	Original Paper
Date Submitted by the Author:	n/a
Complete List of Authors:	rogolino, dominga; University of Parma, dept. of chemistry bacchi, alessia; university of Parma, dept. of chemistry rispoli, gabriele; university of Parma, dept. of chemistry sechi, mario; university of sassari, dept. of chemistry and pharmacy Stevaert, Annelies; Rega Institute for Medical Research, Department of Microbiology and Immunology Naesens, Lieve; Rega Institute for Medical Research, Department of Microbiology and Immunology carcelli, mauro; university of Parma, dept. of chemistry
Keywords:	influenza virus, thiosemicarbazones, endonuclease, magnesium complexes, metal chelation, antiviral



University of Parma
Dipartimento di Chimica
P.co Area delle Scienze 17/A
43124 Parma - ITALY

Tel: +39 0521 905427
Fax: +39 0521 905557
E-mail: mauro.carcelli@unipr.it

February 18, 2015

Manuscript submission

At the attention of
the Editor of *JBIC*

Dear Editor,

In attachment you will find a manuscript entitled "Investigation of the Salicylaldehyde Thiosemicarbazone Scaffold for Inhibition of Influenza Virus PA Endonuclease" which I am submitting for publication in *JBIC* as original Article.

I hope that you and the referees will find the topic suitable for publication. I will be awaiting your response and recommendations.

Yours sincerely,

Prof. Mauro Carcelli
Dept. of Chemistry
University of Parma
P.co Area delle Scienze 17/A
43124 Parma, ITALY
E-mail: mauro.carcelli@unipr.it

Manuscript title:

Investigation of the Salicylaldehyde Thiosemicarbazone Scaffold for Inhibition of Influenza Virus PA Endonuclease

Manuscript category: Original Paper

Manuscript significance: metal chelation has emerged as an efficient strategy to develop new inhibitors of metal-dependent viral enzymes, and, in particular, development of chelating agents targeting the endonuclease active site of RNA-dependent RNA polymerase of influenza virus may represent a successful strategy to tackle influenza infections. Reported endonuclease inhibitors are assumed to chelate the divalent metal ion(s) (Mg^{2+} or Mn^{2+}) in the enzyme's catalytic site, which is located in the N-terminal part of PA (PA-Nter). Here we present a series of salicylaldehyde thiosemicarbazone derivatives evaluated for their ability to inhibit the PA-Nter catalytic activity, highlighting some structure-activity relations. Since chelation may represent a mode of action of such class of molecules, we studied the interaction of two of them, one with and one without biological activity *versus* the PA enzyme, towards Mg^{2+} , the ion that is probably involved in the endonuclease activity of the heterotrimeric influenza polymerase complex. The crystal structure of the magnesium complex of one of the studied inhibitors is also described.

1
2
3
4
5
6
7
8
9
10
11
12
13
14
15
16
17
18
19
20
21
22
23
24
25
26
27
28
29
30
31
32
33
34
35
36
37
38
39
40
41
42
43
44
45
46
47
48
49
50
51
52
53
54
55
56
57
58
59
60

Investigation of the Salicylaldehyde Thiosemicarbazone Scaffold for Inhibition of Influenza Virus PA Endonuclease

Dominga Rogolino·Alessia Bacchi·Gabriele Rispoli·Mario Sechi·Annelies Stevaert·Lieve
Naesens·Mauro Carcelli

Dominga Rogolino·Alessia Bacchi·Gabriele Rispoli·Mauro Carcelli (✉)

Dipartimento di Chimica, Università di Parma, Parco Area delle Scienze 17/A, 43124 Parma, Italy

Email: mauro.carcelli@unipr.it

Mario Sechi

Dipartimento di Chimica e Farmacia, Università di Sassari, Via Vienna 2, 07100 Sassari, Italy

Annelies Stevaert·Lieve Naesens

Rega Institute for Medical Research, KU Leuven, B-3000 Leuven, Belgium

ABSTRACT

The influenza virus PA endonuclease is an attractive target for the development of novel anti-influenza virus therapeutics, which are urgently needed because of the emergence of drug-resistant viral strains. Reported PA inhibitors are assumed to chelate the divalent metal ion(s) (Mg^{2+} or Mn^{2+}) in the enzyme's catalytic site, which is located in the N-terminal part of PA (PA-Nter). In the present work, a series of salicylaldehyde thiosemicarbazone derivatives have been synthesized and evaluated for their ability to inhibit the PA-Nter catalytic activity.

Compounds **1-6** have been evaluated against influenza virus, both in enzymatic assays with influenza virus PA-Nter and in virus yield assays in MDCK cells. In order to establish a structure-activity relationship, the hydrazone analogue of the most active thiosemicarbazone has also been evaluated.

Since chelation may represent a mode of action of such class of molecules, we studied the interaction of two of them, one with and one without biological activity *versus* the PA enzyme, towards Mg^{2+} , the ion that is probably involved in the endonuclease activity of the heterotrimeric influenza polymerase complex. The crystal structure of the magnesium complex of the *o*-vanillin thiosemicarbazone ligand **1** is also described.

Keywords: *influenza virus·thiosemicarbazones·endonuclease·magnesium complexes·metal chelation·antiviral.*

INTRODUCTION

Currently available antiviral drugs to treat or prevent influenza infections comprise two classes of agents: those targeting the viral M2 ion-channel (amantadine and rimantadine) and those targeting the viral neuraminidase (NA) (zanamivir and oseltamivir). The M2 inhibitors have limited clinical

1
2
3 1 utility because of worldwide spread of drug-resistant mutant viruses among almost all influenza A
4
5 2 virus subtypes, including the 2009 pandemic H1N1 virus (1-3). Resistance is also a growing
6
7 3 concern for oseltamivir (4). Therefore, there is an urgent need for entirely novel antiviral
8
9 4 compounds with a different mode of action and targeting a critical step in the viral replication
10
11 5 process (5). The influenza virus genome consists of eight single-stranded (-)RNA segments, which
12
13 6 are transcribed and replicated by the viral RNA-dependent RNA polymerase (RdRp) (6,7). This
14
15 7 RdRp is widely recognized as a superior target for the development of new antivirals, since it is
16
17 8 highly conserved among influenza A, B, and C viruses, and its functions are essential for viral
18
19 9 genome replication (8). It is composed of three subunits: PA, PB1, and PB2. The endonuclease
20
21 10 activity, which resides in the N-terminal part of PA (PA-Nter) (9, 10), is required to cleave host cell
22
23 11 pre-mRNAs and produce the 5'-capped primers for transcription of the viral genomic RNA into
24
25 12 mRNA (cap-snatching) (11). Cap-snatching is an important event in the life cycle of all members of
26
27 13 the *Orthomyxoviridae* family of viruses, including influenza A, B and C viruses. The host cell has
28
29 14 no analogous activity, therefore inhibitors of cap-snatching may be active against all influenza virus
30
31 15 (sub)types and strains, including oseltamivir-resistant influenza viruses, without interfering with
32
33 16 normal host cell functions.

34
35
36
37
38 17 Several X-ray crystallographic studies have been performed on PA-Nter, revealing the presence of
39
40 18 one (10,12) or two (9, 13, 14) divalent metal ions within the active site (**Figure 1**). The two-metal-
41
42 19 ion model is also consistent with biochemical (15) and computational (16) findings. The ions
43
44 20 identified by means of X-ray diffraction are magnesium(II) or manganese(II), depending on the
45
46 21 crystallization conditions. Considering the relative abundance of these two metal ions in the cell
47
48 22 ($[Mg^{2+}]$ is about 1000 times higher than $[Mn^{2+}]$), magnesium may be more biologically relevant.
49
50
51
52
53
54
55
56
57
58
59
60

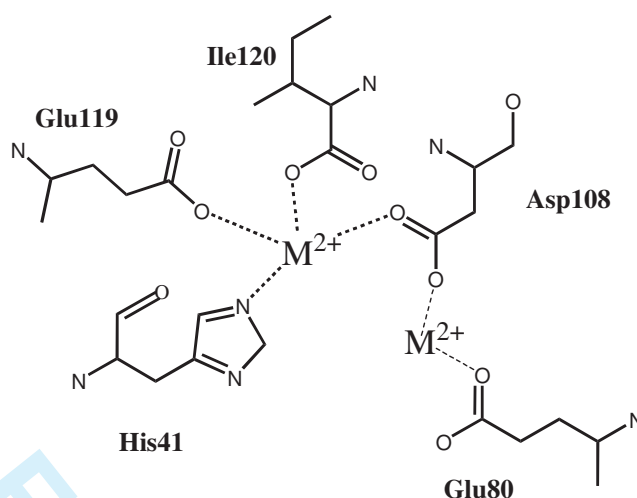


Figure 1. Schematic representation of the metal-interacting residues within the catalytic site of influenza virus PA endonuclease, assuming the presence of two metal ions (see ref. [12] and [13]).

Metal chelation has emerged as an efficient strategy to develop new inhibitors of metal-dependent viral enzymes, the most illustrious example being the class of HIV integrase inhibitors, some of which have already been approved (17). In the same way, development of PA-binding agents with metal-chelating properties may represent a successful strategy to tackle influenza infections. Several chelating molecules have been identified as influenza endonuclease inhibitors, including 2,4-dioxobutanoic acid derivatives (18-20), 5-hydroxy-1,6-dihydropyrimidine-4-carboxylic acids (12), flutimide and its derivatives (21), 2-hydroxyphenyl amide derivatives (22) as well as tetramic acids (23) and 5-hydroxy pyrimidin-4-one derivatives (24) (**Figure 2**).

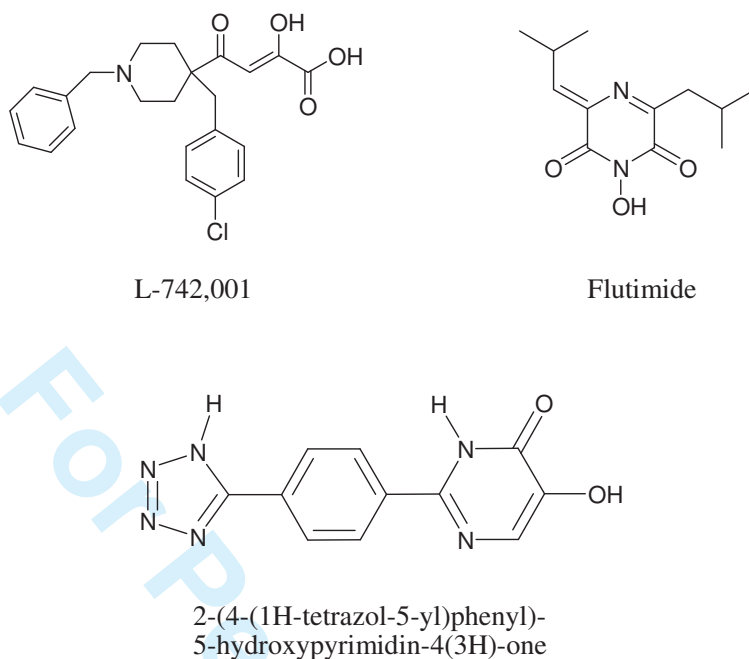
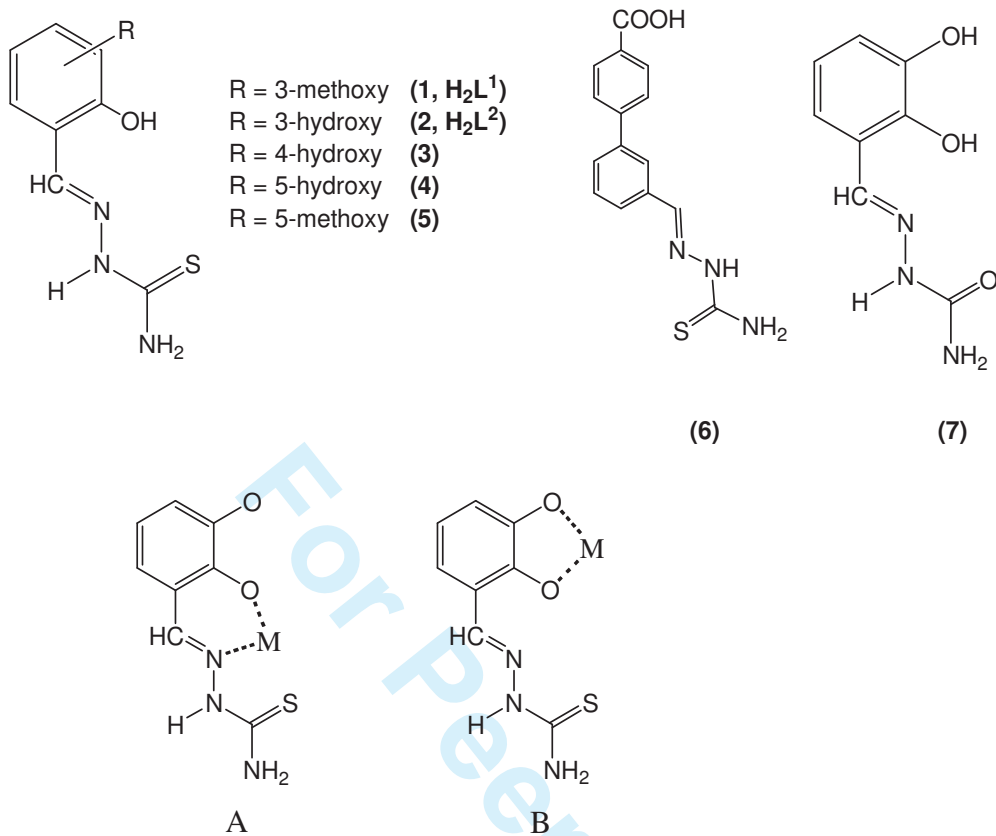


Figure 2. Chemical structures of some prototype inhibitors of influenza virus endonuclease ([19], [21], [24])

Thiosemicarbazones (TSCs) possess a broad range of biological properties including antitumor, antimalarial and antimicrobial activity (25); moreover, they have shown good antiviral activity against herpes simplex virus (26), vaccinia and cowpox virus (27), as well as HIV (28, 29). The biological properties of TSCs are often related to chelation of metal ions (30) and therefore they could be good candidates as chelating inhibitors of influenza virus endonuclease. TSCs can coordinate to the metal centre in an N,S-bidentate mode, but when an additional coordinating group is present, more diversified binding modes become possible (31). In particular, the presence of the OH group in salicylaldehyde thiosemicarbazone derivatives might provide a more favourable coordination for hard metal ions like Mg^{2+} , that prefers oxygen donor atoms.

1
2
3 1 In the present work, we report the synthesis of some salicylaldehyde thiosemicarbazone derivatives (**1**-
4
5 2 **6, Figure 3**) and their biological evaluation against influenza virus, both in enzymatic assays with
6
7 3 influenza virus PA-Nter and in virus yield assays in MDCK cells. In order to investigate the role of the
8
9 4 thiosemicarbazone moiety on activity, we also synthesised and tested compound **7**, the hydrazone
10
11 5 analogue of **2**, the most active molecule in the thiosemicarbazone series.

12
13
14 6 To assess the role of metal chelation in their antiviral mode of action, we have selected **1** and **2** (**1**
15
16 7 without activity and **2** with reasonable activity against the PA-Nter enzyme) and studied their
17
18 8 interactions with Mg^{2+} , the ion that is probably involved in the endonuclease activity of the native
19
20 9 influenza virus RdRp complex. Finally, the crystal structure of complex $Mg(HL^1)_2 \cdot 2CH_3OH$ is
21
22 10 described (**1**, H_2L^1).
23
24
25
26
27
28
29
30
31
32
33
34
35
36
37
38
39
40
41
42
43
44
45
46
47
48
49
50
51
52
53
54
55
56
57
58
59
60



1

2 **Figure 3.** Chemical structures of ligands 1-7 and the coordination modes A and B of 1-5, involving
3 the OH groups.

1

2 **Materials and methods**

3

4 Chemistry

5

6 All reagents of commercial quality were used without further purification. Purity of compounds was
7 determined by elemental analysis and verified to be $\geq 95\%$ for all synthesized molecules. NMR
8 spectra were recorded at 25 °C on a Bruker Avance 400 FT spectrophotometer. The ATR-IR
9 spectra were recorded by means of a Nicolet-Nexus (Thermo Fisher) spectrophotometer by using a
10 diamond crystal plate in the range of 4000-400 cm^{-1} . Elemental analyses were performed by using a
11 FlashEA 1112 series CHNS/O analyzer (Thermo Fisher) with gas-chromatographic separation.
12 Electrospray mass spectral analyses (ESI-MS) were performed with an electrospray ionization (ESI)
13 time-of-flight Micromass 4LCZ spectrometer. MS spectra were acquired in positive EI mode by
14 means of a DEP-probe (Direct Exposure Probe) mounting on the tip a Re-filament with a DSQII
15 Thermo Fisher apparatus, equipped with a single quadrupole analyzer.

16 **Synthesis of the ligands.** The TSCs **1-6** and hydrazone **7** were prepared following reported
17 procedures (32). Briefly, to a solution of the aldehyde in absolute ethanol, an equimolar amount of
18 thiosemicarbazide was added, dissolved in the same solvent. In the synthesis of **7**, semicarbazide
19 hydrochloride was used, which was suspended in ethanol and the pH adjusted to 7 by using KOH
20 1M. The mixture was refluxed for 6 hours, cooled at room temperature and concentrated in vacuum.
21 The resulting precipitate was filtered off, washed with cold ethanol and dried in vacuum.

22 **N-(2-hydroxy-3-methoxybenzylidene)-thiosemicarbazide (1, H₂L¹).** Yield = 71%. ¹H-NMR
23 (DMSO-d₆, 25°C), δ : 3.80 (s, 3H, OCH₃), 6.77 (t, 1H; J = 7.9 Hz, ArH), 6.96 (d, 1H, J = 7.8 Hz,
24 ArH), 7.52 (d, 1H, J = 7.8 Hz, ArH), 7.87 (s, br, 1H, NH), 8.09 (s, br, 1H, NH), 8.40 (s, 1H;
25 HC=N), 9.20 (s, br, 1H, OH), 11.39 (s, br, 1H; NH). ¹H-NMR (MeOD-d₄, 25°C), δ : 3.90 (s, 3H,

1
2
3
4
5
6
7
8
9
10
11
12
13
14
15
16
17
18
19
20
21
22
23
24
25
26
27
28
29
30
31
32
33
34
35
36
37
38
39
40
41
42
43
44
45
46
47
48
49
50
51
52
53
54
55
56
57
58
59
60

1 OCH₃), 6.84 (t, 1H; J = 7.9 Hz, ArH), 6.99 (d, 1H, J = 7.8 Hz, ArH), 7.43 (d, 1H, J = 7.8 Hz, ArH),
2 8.41 (s, 1H; HC=N). MS (EI, 70 eV), m/z (%) = 225.0 ([M]⁺, 100); IR (cm⁻¹): ν_{NH} = 3459, 3339;
3 ν_{OH} = 3158 (br); ν_{C=N} = 1596; ν_{C=S} = 1532, 821; ν_{OCH₃} = 1258, 1056. Anal. Calcd. for
4 C₉H₁₁N₃O₂S·0.5H₂O: C 46.14; H 5.16; N 17.94. Found: C 45.92, H 4.82, N 18.24.

5 **N-(2,3-dihydroxybenzylidene)-thiosemicarbazide (2, H₂L²)**. Yield = 75%. ¹H-NMR (DMSO-d₆,
6 25°C), δ: 6.63 (t, 1H; J = 7.9 Hz, ArH), 6.79 (d, 1H, J = 7.8 Hz, ArH), 7.35 (d, 1H, J = 7.5 Hz,
7 ArH), 7.86 (s, br, 1H, NH), 8.08 (s, br, 1H, NH), 8.36 (s, 1H; HC=N), 9.20 (s, vbr, 2H, OH), 11.37
8 (s, br, 1H; NH). ¹H-NMR (MeOD-d₄, 25°C), δ: 6.75 (t, J = 7.9 Hz, 1H), 6.86 (dd, J = 7.9, 1.6 Hz,
9 1H), 7.14 (d, J = 7.9 Hz, 1H), 8.30 (s, 1H, HC=N). MS (EI, 70 eV), m/z (%) = 210.9 ([M]⁺, 100);
10 IR (cm⁻¹): ν_{NH} = 3364, 3256; ν_{OH} = 3173 (br); ν_{C=N} = 1620; ν_{C=S} = 1539, 825. Anal. Calcd. for
11 C₈H₉N₃O₂S·0.5H₂O: C 43.63; H 4.58; N 19.08. Found: C 43.33, H 4.48, N 18.98.

12 **N-(2,4-dihydroxybenzylidene)-thiosemicarbazide (3)** Yield = 78%. ¹H-NMR (DMSO-d₆, 25°C),
13 δ: 6.25-6.29 (m, 2H; ArH), 7.67 (d, 1H, J = 8.4 Hz, ArH), 7.74 (s, br, 1H, NH), 7.94 (s, br, 1H,
14 NH), 8.24 (s, 1H; HC=N), 9.78 (s, br, 2H, OH), 11.17 (s, br, 1H; NH). MS (EI, 70 eV), m/z (%) =
15 211.0 ([M]⁺, 100); IR (cm⁻¹): ν_{NH} = 3479, 3347; ν_{OH} = 3262, 3128 (br); ν_{C=N} = 1630; ν_{C=S} = 1582,
16 875. Anal. Calcd. for C₈H₉N₃O₂S·1/3H₂O: C 44.23; H 4.48; N 19.34. Found: C 43.94, H 4.05, N
17 19.18.

18 **N-(2,5-dihydroxybenzylidene)-thiosemicarbazide (4)** Yield = 85%. ¹H-NMR (DMSO-d₆, 25°C),
19 δ: 6.68 (m, 2H; ArH), 7.22 (s, 1H, ArH), 7.78 (s, br, 1H, NH), 8.07 (s, br, 1H, NH), 8.30 (s, 1H;
20 HC=N), 8.83 (s, br, 2H, OH), 9.21 (s, br, 2H, OH), 11.33 (s, br, 1H; NH). MS (EI, 70 eV), m/z (%)
21 = 211.0 ([M]⁺, 100); IR (cm⁻¹): ν_{NH} = 3427, 3328; ν_{OH} = 3048, 3002 (br); ν_{C=N} = 1623; ν_{C=S} = 1559,
22 942. Anal. Calcd. for C₈H₉N₃O₂S·1/3H₂O: C 44.23; H 4.48; N 19.34. Found: C 44.11, H 4.39, N
23 19.18.

24 **N-(2-hydroxy-5-methoxybenzylidene)-thiosemicarbazide (5)** Yield = 63%. ¹H-NMR (DMSO-d₆,
25 25°C), δ: 6.76-6.84 (m, 2H; ArH), 7.48 (s, 1H, ArH), 8.01 (s, br, 1H, NH), 8.13 (s, br, 1H, NH),
26 8.35 (s, 1H; HC=N), 9.44 (s, br, 2H, OH), 11.36 (s, br, 1H; NH). MS (EI, 70 eV), m/z (%) = 225.0

1
2
3 1 ([M]⁺, 100); IR (cm⁻¹): ν_{NH} = 3412, 3304; ν_{OH} = 3120 (br); ν_{C=N} = 1626; ν_{C=S} = 1537, 821. Anal.
4
5 2 Calcd. for C₉H₁₁N₃O₂S: C 47.99; H 4.92; N 18.65. Found: C 48.17, H 4.82, N 18.34.

6
7 3 **N-(3-(1,1'-biphenyl)-4-carboxylic acid)-thiosemicarbazide (6)**. Yield = 51%. ¹H-NMR (DMSO-
8
9 4 d₆, 25°C), δ: 7.53 (t, J = 8 Hz, 1H; ArH), 7.78 (m, 2H, ArH), 7.89 (d, J = 8 Hz, 2H, ArH), 8.03 (d,
10
11 5 2H, ArH), 8.13-8.26 (m, 4H, ArH+HC=N+NH₂), 11.51 (s, br, 1H, NH), 13.00 (s, br, 1H, OH). MS
12
13 6 (EI, 70 eV), m/z (%) = 298.9 ([M]⁺, 60); IR (cm⁻¹): ν_{NH+OH} = 3432, 3263, 3143 (br); ν_{C=N} = 1606;
14
15 7 ν_{NH2} = 1535. Anal. Calcd. for C₂₁H₁₆N₂O₆S·1.5H₂O: C 55.21; H 4.94; N 12.88. Found: C 55.38, H
16
17 8 4.85, N 13.03.

18
19
20 9 **N-(2,3-dihydroxybenzylidene)-semicarbazide (7)**. Yield = 70%. ¹H-NMR (DMSO-d₆, 25°C), δ:
21
22 10 6.36 (s, br, 2H, NH₂), 6.64 (t, 1H; J = 7.9 Hz, ArH), 6.76 (d, 1H, J = 7.8 Hz, ArH), 7.17 (d, 1H, J =
23
24 11 7.5 Hz, ArH), 8.14 (s, 1H; HC=N), 9.21, 9.39 (s, br, 2H, OH), 10.17 (s, br, 1H; NH). ¹H-NMR
25
26 12 (MeOD-d₄, 25°C), δ: 6.75 (t, J = 7.9 Hz, 1H), 6.86 (dd, J = 7.9, 1.6 Hz, 1H), 7.14 (d, J = 7.9 Hz,
27
28 13 1H), 8.30 (s, 1H, HC=N). MS (EI, 70 eV), m/z (%) = 195.0 ([M]⁺, 100); IR (cm⁻¹): ν_{NH} = 3455,
29
30 14 3350; ν_{OH} = 3166 (br); ν_{C=O} = 1694; ν_{C=N} = 1592. Anal. Calcd. for C₈H₉N₃O₃: C 49.23; H 4.65; N
31
32 15 21.53. Found: C 49.16, H 4.48, N 21.40.

33
34
35 16 **Mg(HL¹)₂ · 2.5 H₂O (8)**. 0.5 mmol of H₂L¹ was dissolved in 20 ml of methanol and 4 eq. of NEt₃
36
37 17 were added. The solution turned yellow and it was stirred at r.t. for 30 minutes; 0.5 eq. of
38
39 18 magnesium acetate were added and the reaction mixture was stirred at r.t. for 4 hours, concentrated
40
41 19 in vacuum and cooled overnight. The precipitate was filtered off and washed with water. Crystals
42
43 20 suitable for X-ray diffraction analysis were obtained by slow evaporation of the mother liquors at
44
45 21 room temperature. Yield: 74%. ¹H-NMR (MeOD, 25°C), δ: 3.89 (s, 3H, OCH₃); 6.84 (t, br, 1H,
46
47 22 ArH), 6.98 (d, br, 1H, ArH), 7.42 (d, br, 1H, ArH), 8.40 (s, 1H, HC=N). MS-ESI, m/z (+,%) = 473
48
49 23 ([M+H]⁺, 40); 495 ([M+Na]⁺, 40). IR (cm⁻¹): ν_{NH} = 3334 (br); ν_{C=N} = 1596; ν_{C=S} = 1534; ν_{OCH3}
50
51 24 =1238, 1027. Anal. Calcd. for C₁₈H₂₀N₆O₄Mg · 2.5H₂O: C 41.75, H 4.87, N 16.23, S 12.38. Found:
52
53 25 C 41.30, H 4.75, N 16.12, S 12.97.

1
2
3 1 **Mg(HL²)₂ (9)**. 0.5 mmol of H₂L² was dissolved in 20 ml of degassed methanol under nitrogen and 4
4
5 2 eq. of NEt₃ were added. The solution turned yellow and it was stirred at r.t. for 30 minutes; 0.5 eq.
6
7 3 of magnesium acetate were added and the reaction mixture was stirred at r.t. for 4 hours,
8
9 4 concentrated in vacuum and cooled overnight. The precipitate was filtered off under inert
10
11 5 atmosphere, washed with water and kept under nitrogen. Both the solution and the solid turn dark if
12
13 6 exposed to air. ¹H-NMR (MeOD-d₄, 25°C), δ: 6.47 (s, br, 2H), 6.81 (s, br, 1H), 8.12 (s, br, 1H,
14
15 7 HC=N). MS-ESI, m/z (-, %) = 443 ([M]⁻, 10); 210 ([HL²]⁻, 100). IR (cm⁻¹): ν_{NH+OH} = 3275, 3164
16
17 8 (br); ν_{C=N} = 1568; ν_{C=S} = 1534.
18
19
20
21 9

10 **X-ray crystallography**

11
12 Single crystals of **2** and of **Mg(HL¹)₂·2CH₃OH** were selected and mounted on glass fibers to collect
13
14 data on a SMART Breeze diffractometer. The crystals were kept at 293 K during data collection.
15
16 **Table 1** reports crystal data and structure analysis. Using Olex2 (33), the structure was solved with
17
18 the SIR2004 (34) structure solution program using Direct Methods and refined with the ShelXL
19
20 refinement package (35) using Least Squares minimisation. Anisotropic displacement parameters
21
22 were refined for all non-hydrogen atoms. Hydrogen atoms were partly located on the Fourier
23
24 difference map and partly introduced in calculated positions riding on their carrier atoms. Hydrogen
25
26 bonds were analyzed with PARST97 (36) and the Cambridge Structural Database software (37,38)
27
28 was used for the analysis of the crystal packing. **Table 1** summarizes crystal data and structure
29
30 determination results. Crystallographic data (excluding structure factors) for **2** and
31
32 **Mg(HL¹)₂·2CH₃OH** have been deposited with the Cambridge Crystallographic Data Centre as
33
34 supplementary publication no. CCDC 1049845-1049846. Copies of the data can be obtained free of
35
36 charge on application to CCDC, 12 Union Road, Cambridge CB2 1EZ, UK (fax: (+44) 1223-336-
37
38 033; e-mail: deposit@ccdc.cam.ac.uk).

Biology

Production of recombinant influenza virus PA-Nter protein

The coding sequence for PA-Nter (i.e., residues 1-217 from the PA protein of influenza virus strain A/X-31) was cloned in the pET28a(+) plasmid (Merck KGaA, Darmstadt, Germany) with an N-terminal 6xHis-tag, and this bacterial expression plasmid was transformed into *E. coli* BL21-CodonPlus cells (Agilent Technologies, Santa Clara, CA). These bacteria were grown to an OD of 0.6, when IPTG was added at a final concentration of 1 mM to induce expression of recombinant protein for 5 h at 37 °C. The bacterial cells were ruptured using a French press and the protein was purified by 6xHis-Ni-NTA chromatography (Qiagen, Valencia, CA), followed by buffer exchange using PD-10 desalting columns (GE Healthcare, Diegem, Belgium) to keep the protein in storage buffer (50 mM Tris-HCl pH 8, 100 mM NaCl, 10 mM β -mercaptoethanol, 50% glycerol). Protein purity was verified by SDS-PAGE with Coomassie Blue staining, and protein concentration was determined by Bradford assay. Finally, the purified protein was divided in aliquots and stored at -80 °C.

Plasmid-based endonuclease assay

The enzymatic PA-Nter assay was performed according to a published method (22) with minor modifications (20). One microgram of recombinant PA-Nter was incubated with 1 μ g (16.7 nM) of single-stranded circular DNA plasmid M13mp18 (Bayou Biolabs, Metairie, Louisiana) in the presence of the test compounds and at a final volume of 25 μ L. The assay buffer contained 50 mM Tris-HCl pH 8, 100 mM NaCl, 10 mM β -mercaptoethanol and 1 mM $MnCl_2$. The reaction was incubated at 37 °C for 2 h and then stopped by heat inactivation (80 °C, 20 min). The endonucleolytic digestion of the plasmid was visualized by gel electrophoresis on a 1% agarose gel

1
2
3
4
5
6
7
8
9
10
11
12
13
14
15
16
17
18
19
20
21
22
23
24
25
26
27
28
29
30
31
32
33
34
35
36
37
38
39
40
41
42
43
44
45
46
47
48
49
50
51
52
53
54
55
56
57
58
59
60

1 with ethidium bromide staining, and the amount of remaining intact plasmid was quantified by
2 ImageQuant TL software (GE Healthcare).

3 The percentage inhibition of endonuclease activity was plotted against the compound concentration
4 on a semi-logarithmic plot, using GraphPad Prism software (GraphPad Software, La Jolla, CA).
5 Values were the mean \pm S.E.M. of three independent experiments. The 50% inhibitory
6 concentrations (IC₅₀) were obtained by nonlinear least squares regression analysis. The known PA-
7 Nter inhibitor 2,4-dioxo-4-phenylbutanoic acid (DPBA) was included as the reference compound.

8 9 Cells and media

10
11 Madin-Darby canine kidney (MDCK) cells (a kind gift from M. Matrosovich, Marburg, Germany)
12 and human embryonic kidney 293T (HEK293T) cells (purchased from Thermo Scientific) were
13 grown in Dulbecco's modified Eagle medium (DMEM) supplemented with 10% fetal calf serum
14 (FCS), 1 mM sodium pyruvate and 0.075% sodium bicarbonate. Virus experiments were performed
15 in MDCK infection medium, consisting of Ultra MDCK medium (Lonza, Basel, Switzerland)
16 supplemented with 0.0225% sodium bicarbonate, 2 mM L-glutamine, and 2 μ g/mL tosyl
17 phenylalanyl chloromethyl ketone (TPCK)-treated trypsin (Sigma-Aldrich). The cells were
18 incubated in a 5% CO₂ humidified atmosphere.

19 20 vRNP reconstitution assay

21
22 The assay to determine the inhibitory effect of the compounds on reconstituted influenza virus
23 vRNPs is described in more detail elsewhere (39, 40). Briefly, the four relevant expression plasmids
24 derived from influenza A/PR/8/34 [i.e., pVP-PB1, pVP-PB2, pVP-NP, and pVP-PA; generously
25 donated by M. Kim (41), Korea Research Institute of Chemical Technology, Daejeon, South Korea]
26 were combined with a firefly luciferase reporter plasmid (also a kind gift from M. Kim) and

1
2
3 1 cotransfected into HEK293T cells using Lipofectamine 2000. After 24 h incubation at 37 °C in the
4
5 2 presence of the test compounds, luciferase activity was determined using the ONE-Glo luciferase
6
7 3 assay system (Promega). The 50% effective concentration (EC₅₀) was defined as the compound
8
9 4 concentration causing 50% reduction in the vRNP-driven firefly luciferase signal, as compared to
10
11 5 cells receiving medium instead of compound. These EC₅₀ values were calculated by interpolation
12
13 6 assuming a semi-log dose-response effect. In parallel, the compound cytotoxicity, expressed as
14
15 7 CC₅₀ (50% cytotoxic concentration) was determined using the spectrophotometric MTS cell
16
17 8 viability assay (CellTiter 96 AQueous One Solution Cell Proliferation Assay; Promega). The CC₅₀
18
19 9 values were defined as the compound concentration reducing cell viability in untransfected
20
21 10 HEK293T cells by 50%, as compared to the wells receiving medium instead of compound.
22
23 11 Ribavirin was included as the reference compound.
24
25
26
27
28
29
30
31
32
33

34 13 Virus yield assay

35
36 14 To determine anti-influenza virus activity in cell culture, a virus yield assay was performed (40).
37
38 15 One day prior to infection, MDCK cells were seeded into 96-well plates at 25,000 cells per well. At
39
40 16 day 0, the test compounds were added at serial dilutions, immediately followed by infection with
41
42 17 influenza A/PR/8/34 virus. The multiplicity of infection (MOI) was 150 CCID₅₀ per well (50% cell
43
44 18 culture infectious dose; determined by the method of Reed and Muench (42)). After 24 h incubation
45
46 19 at 35 °C, the supernatants were harvested and stored at -80 °C. The viral copy number in these
47
48 20 samples was estimated by a one-step quantitative real-time reverse transcription (qRT)-PCR assay
49
50 21 (CellsDirect One-Step qRT-PCR kit; Invitrogen, Life Technologies, Gent, Belgium), with influenza
51
52 22 virus M1-specific primers and probe [see (43) for all details]. An M1-plasmid standard was
53
54 23 included to allow absolute quantification. The EC₉₉ and EC₉₀ values were calculated by
55
56 24 interpolation from data of at least three experiments and defined as the compound concentration
57
58 25 causing respectively a 2-log₁₀ and 1-log₁₀ reduction in viral RNA (vRNA) copy number, as
59
60 26

1
2
3 1 compared to the virus control receiving no compound. In parallel, uninfected MDCK cells were
4
5 2 used to determine the CC_{50} values of the compounds after 24 h incubation, using the MTS cell
6
7 3 viability assay (CellTiter 96 AQueous One Solution Cell Proliferation Assay; Promega). Ribavirin
8
9 4 was included as the reference compound.
10

11 5 12 6 **Results and discussion**

13 7 14 8 **Chemistry**

15 9
16 10 The ligands **1-6** (**Figure 3**) were easily prepared in high yields by condensation of the
17 11 thiosemicarbazide and the substituted benzaldehyde; they were characterized by spectroscopic
18 12 tools, mass spectrometry and elemental analysis. **2** was also characterized by single crystal X-ray
19 13 diffraction. In **6** the OH/OCH₃ groups are substituted by a carboxylic moiety, which retains good
20 14 affinity for magnesium ions, following a suggestion emerged in the research for new inhibitors of
21 15 HIV RNase H (44), which has two magnesium ions in its active site. In the IR spectra of **1-6** the
22 16 C=S stretching absorptions are at about 1530-1580 and 820-940 cm^{-1} ; in the ¹H-NMR spectra, the
23 17 resonances of the iminic proton (about 8.0 ppm) and of the hydrazonic NH and of NH₂ (11.3 ppm
24 18 and 7.8-8.0 ppm, approximately) are evident. Isomerism around the C=N bond is possible, but in
25 19 the ¹H-NMR spectra registered in d₆-DMSO there is only one set of signals: evidently, all the
26 20 ligands are in the *E* form in solution. Even if these ligands can give rise to a thione-thiol
27 21 equilibrium, no evidence was obtained about the presence of the thiolic form in solution. Analogous
28 22 considerations can be made for **7**, the hydrazonic analogue of compound **2**.

29 23 Ligands **1-5** are very versatile: they possess both soft and hard donor atoms and they can act as
30 24 bidentate or tridentate chelating ligands. Complexes of salicylaldehyde thiosemicarbazones with
31 25 divalent metals like Pd(II), Zn(II), Cu(II), Ni(II) have been studied previously (45-50), but little is
32 26 known about their interactions with magnesium ions (51). Magnesium is a hard Lewis acid and so

1
2
3 1 coordination of the sulphur atom could be excluded. It is known that salicylaldimine ligands can be
4
5 2 NO-coordinated to magnesium (A, **Figure 3**), but in **1** and **2**, with two oxygen donors in *ortho*,
6
7 3 coordination B (**Figure 3**) is also plausible. Since chelation of the divalent metal cofactors within
8
9 4 the active site of the influenza virus PA endonuclease provides the possible basis for their antiviral
10
11 5 activity (17), we decided to clarify the coordination properties of two of these ligands (**1** and **2**,
12
13 6 H_2L^1 and H_2L^2 , respectively) towards Mg^{2+} . The ligands were combined with magnesium acetate to
14
15 7 react in the presence of triethylamine as a base to afford the corresponding metal complexes **8** and
16
17 8 **9**. It is worth noting that, in the case of **2**, the reaction was executed under inert atmosphere, since
18
19 9 the reaction mixture became dark when exposed to air. In order to verify the influence of the metal
20
21 10 to ligand *ratio* or the pH, different reaction conditions were used with **1** (1:1 and 1:2 metal to ligand
22
23 11 *ratio*; up to 4 equivalents of base), but only with a 1:2 metal to ligand *ratio* and in the presence of 4
24
25 12 equivalents of base, a metal complex was isolated.

26
27 13 The infrared spectrum of both **8** and **9** displays bands associated to the NH group ($3163\text{-}3460\text{ cm}^{-1}$),
28
29 14 thus indicating that this functionality is not deprotonated. The bands associated to the C=S
30
31 15 stretching are unaffected upon complexation, therefore it can be assumed that this group is not
32
33 16 involved in coordination, as confirmed by X-ray diffraction analysis on **8**. In the IR spectrum of **8**
34
35 17 the stretching of the methoxy group is slightly shifted compared to the free ligand, suggesting a
36
37 18 possible involvement in coordination. The 1H -NMR spectrum of **8** registered in d_6 -DMSO shows
38
39 19 the presence of two sets of signals: one set corresponds to the free ligand, while the second one
40
41 20 corresponds to the metal complex. The use of a coordinating solvent, therefore, causes the partial
42
43 21 decoordination of the ligand. On the contrary, in the 1H -NMR spectrum in MeOD, where the
44
45 22 solubility is however low, there is a unique set of signals: the ligand coordinates to the metal in a
46
47 23 bidentate fashion only when a poor coordinating solvent is present. The 1H -NMR spectrum of **9**
48
49 24 shows very broad signals, which might indicate that a fluxional behavior can exist in solution. It is
50
51 25 worth noting that complex **9** is not stable if exposed to air both in solution and at the solid state.
52
53
54
55
56
57
58
59
60

1
2
3
4
5
6
7
8
9
10
11
12
13
14
15
16
17
18
19
20
21
22
23
24
25
26
27
28
29
30
31
32
33
34
35
36
37
38
39
40
41
42
43
44
45
46
47
48
49
50
51
52
53
54
55
56
57
58
59
60

1 Mass spectra confirmed the presence in solution of complexes of type $M(HL)_2$ and elemental
2 analysis confirmed the proposed stoichiometry, $Mg(HL^1)_2 \cdot 2.5 H_2O$, for **8**.

3
4 X-ray crystallography

5
6 Ligand **2** was crystallized from ethanol as the solvate form $2 \cdot CH_3CH_2OH$ (Table 1). The molecular
7 structure, shown in Figure 4, is perfectly planar, and the thiosemicarbazone chain is completely
8 extended, with *trans* torsion angles larger than 175° along the chain. The *cis* configuration between
9 the amide NH and the imidic CH favours the aggregation of coplanar molecular pairs by the
10 interactions between these groups and the sulphur (Figure 4, bottom) ($N2-H \dots S1(i) = 3.401(1) \text{ \AA}$,
11 $167.2(1)^\circ$, $C7-H \dots S1(i) = 3.762(1) \text{ \AA}$, $152.0(1)^\circ$, $i = 1-x, -y, 2-z$). The dimeric assembly is surrounded
12 by ethanol molecules linked by hydrogen bonds to the hydroxyl groups of **2** which act as donors:
13 $O2-H \dots O3(ii) = 2.816(2) \text{ \AA}$, $141(2)^\circ$; $O1-H \dots O3(iii) = 2.770(2) \text{ \AA}$, $168(3)^\circ$ ($ii = 2-x, y-1/2, 3/2-z$; $iii = 2-$
14 $x, -y, 1-z$). The ethanol molecule in turn donates a hydrogen bond to the sulphur atom ($O3-$
15 $H \dots S1(iv) = 3.218(1) \text{ \AA}$, $158(2)^\circ$, $iv = x+1, y, z$) while the $-NH_2$ moiety donates a hydrogen bond to
16 one hydroxyl group ($N3-H \dots O2(v) = 3.013(2) \text{ \AA}$, $178(2)^\circ$, $v = 1-x, 1/2+y, 3/2-z$), thus generating a
17 three-dimensional hydrogen bond network.

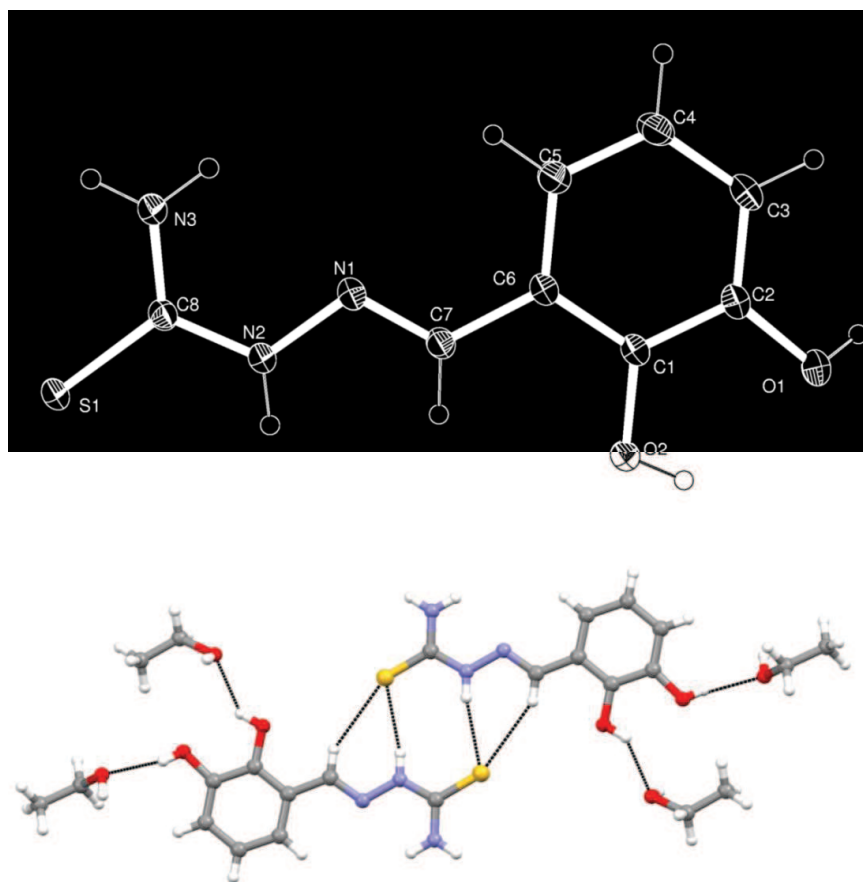


Figure 4. Molecular structure and labelling of **2**, with thermal ellipsoids drawn at the 50% probability level. Bottom: supramolecular aggregation of **2**·CH₃CH₂OH in the solid, with dotted hydrogen bonds.

1
2
3 1
4
5
6 2
7
8 3
9
10 4
11
12 5
13
14 6
15
16 7
17
18
19
20
21
22
23
24
25
26
27
28
29
30
31
32
33
34
35
36
37
38
39
40
41
42
43
44
45
46
47
48
49 8
50
51
52 9
53
54 10
55
56 11
57
58
59
60

Complex $\text{Mg}(\text{HL}^1)_2 \cdot 2\text{CH}_3\text{OH}$ crystallizes from methanol in the orthorhombic $P2_1n$ space group (Table 1). The neutral complex comprises two monodeprotonated $(\text{HL}^1)^-$ ligands coordinated in a bidentate mode to the magnesium cation by means of the methoxy group and of the deprotonated hydroxyl group, forming two planar five-membered chelation rings; two *cis* methanol molecules complete the octahedral coordination (Figure 5) and the overall complex molecule has a pseudo twofold rotation axis relating the two ligands and the two methanol molecules.

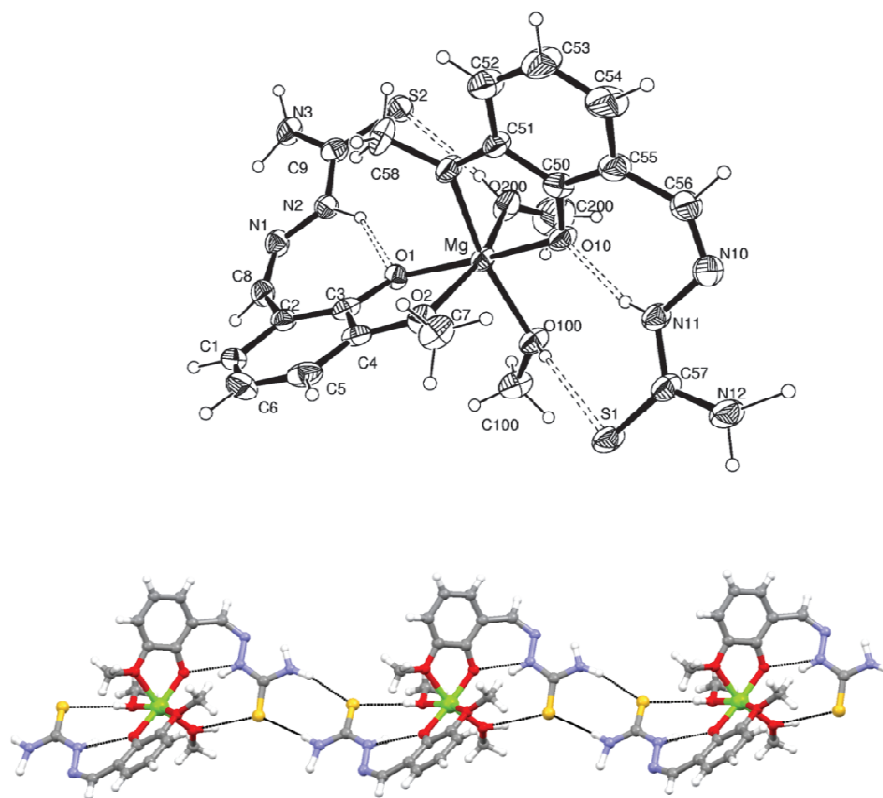


Figure 5. Molecular structure and labelling of complex $\text{Mg}(\text{HL}^1)_2 \cdot 2\text{CH}_3\text{OH}$, with thermal ellipsoids drawn at the 50% probability level and dashed intramolecular hydrogen bonds. Bottom: supramolecular aggregation of $\text{Mg}(\text{HL}^1)_2 \cdot 2\text{CH}_3\text{OH}$ in the solid, with dotted hydrogen bonds.

1
2
3 1
4
5 2 The *mer* configuration of the two bidentate ligand confers optical activity to the complex; the
6
7 3 crystal is however racemic due to the presence of reflection planes. The thiosemicarbazone arms are
8
9 4 protonated on the amidic nitrogen and are noticeably distorted due to intramolecular interactions. In
10
11 5 fact the amide NH and the imidic CH groups are in *trans* configuration, and the latter is also turned
12
13 6 away from the hydroxyl group, in contrast to the situation observed for the free ligand **2** (H_2L^2),
14
15 7 whose molecular structure is comparable to **1** (H_2L^1). The torsion angles along the chains of the two
16
17 8 ligands (HL^1)⁻ in the complex differ significantly from the 0/180° value of the extended
18
19 9 conformation of the free ligand, reported in parentheses: C1-C2-C8-N1= 150/155°(-5°), C2-C8-N1-
20
21 10 N2=7/3° (180°), C8-N1-N2-C9=-166/-162°(175°), N1-N2-C9-N3=9/5°(-2°). These conformational
22
23 11 distortions are mainly due to strong intramolecular hydrogen bonds between the amidic NH and the
24
25 12 coordinated deprotonated hydroxyl oxygens (N2-H...O1=2.582(1)Å, 147(1)°; N11-
26
27 13 H...O10=2.589(1)Å, 153(1)°), and between the coordinated methanol molecules and the sulphur
28
29 14 atoms (O100-H...S1=3.189(1)Å, 155(1)°; O200-H...S2=3.212(1)Å, 159(1)°). The -NH₂ moiety is
30
31 15 involved in an intermolecular hydrogen bond to the sulphur atom generating an R22(8) ring (**Figure**
32
33 16 **5**, bottom) which expands in ribbons along the diagonal *ab* (N3-H...S1(vi)=3.410(1)Å, 162(1)°;
34
35 17 N12-H...S2(vii)=3.503(2)Å, 166(1)°, vi=x+1, y-1, z, vii=x-1, y+1, z). In both the free ligand and the
36
37 18 complex the sulphur atoms are significantly involved in intermolecular interactions where they act
38
39 19 as acceptors from -OH and -NH groups.
40
41
42
43
44
45
46
47
48
49
50
51
52
53
54
55
56
57
58
59
60

21 Biological activity

22
23 Compounds **1-6** were evaluated for their ability to inhibit endonuclease activity in an enzymatic
24
25 assay with recombinant PA-Nter, and the results are presented in **Table 2**. Besides, their anti-
26
27 influenza virus activity was determined in cell culture, in a virus yield assay in MDCK cells and in
28
29 a vRNP reconstitution assay in HEK293T cells. We also evaluated the inhibitory activity of **1-6**

1
2
3
4
5
6
7
8
9
10
11
12
13
14
15
16
17
18
19
20
21
22
23
24
25
26
27
28
29
30
31
32
33
34
35
36
37
38
39
40
41
42
43
44
45
46
47
48
49
50
51
52
53
54
55
56
57
58
59
60

1 against a broad panel of DNA [i.e. herpes simplex virus type 1, vaccinia virus and adenovirus,
2 evaluated in infected human embryonic lung fibroblast (HEL) cells] and RNA viruses (Coxsackie
3 B4 virus and respiratory syncytium virus, tested in HeLa cells; parainfluenza-3 virus and Punta
4 Toro virus, tested in Vero cells). However, they were found to be inactive against these diverse
5 viruses, with the exception of a modest activity of **2** against herpes simplex virus-1 ($EC_{50} = 58 \mu\text{M}$)
6 and vaccinia virus ($EC_{50} = 45 \mu\text{M}$).

7 As can be seen in **Table 2**, compounds **2** and **4** displayed moderate activity in the PA-Nter
8 enzymatic assay, with the catechol derivative **2** presenting the best result (IC_{50} : $37 \mu\text{M}$). It is
9 interesting to note that this compound has an activity profile similar to that of a 2,3-
10 dihydroxyphenyl amide inhibitor that we recently reported (22), indicating the importance of the
11 catechol pharmacophore for inhibition of the PA-Nter enzyme. In line with the enzymatic data on
12 series **1-6**, compounds **2** and **4** were also the only derivatives showing antiviral activity in both cell
13 culture assays. Compound **2** displayed an $EC_{99} \geq 87 \mu\text{M}$ and $EC_{90} \geq 56 \mu\text{M}$ in the virus yield assay,
14 and an EC_{50} value of $63 \mu\text{M}$ in the vRNP reconstitution assay. For **4**, the corresponding values were
15 48, 34 and $22 \mu\text{M}$, respectively. Additionally, compound **5** displayed weak inhibitory activity in the
16 vRNP reconstitution assay, with an average IC_{50} value of $150 \mu\text{M}$.

17 Even if the set of data is quite limited, some careful conclusions can be drawn. **1** and **2** can
18 coordinate the divalent magnesium ion in the B mode, by using the methoxy and OH groups (**1**) or
19 two OH groups (**2**); however, **1** is inactive, while **2** has moderate activity. The same type of
20 substitution, i.e. moving from **4** (5-OH) to **5** (5-methoxy), has the same effect on biological activity
21 [i.e. **4** is moderately active; **5** has very weak activity (vRNP reconstitution assay) or is inactive
22 (virus yield assay)]. It is difficult to correlate this effect to a different coordinating ability of the
23 ligands, in particular looking at **4** and **5**, which can both use mode A (**Figure 3**). Similarly, a
24 different coordination behaviour cannot explain the different activity of **3** and **4**. On the other hand,

1
2
3 1 the finding that **4** has lower activity in the enzymatic assay than **2**, could well be related to their
4
5 2 different coordination mode to the magnesium ion in the active site of the PA-Nter enzyme.
6

7 3 To further investigate the role of the thiosemicarbazone moiety on activity, we evaluated the
8
9 4 biological activity of compound **7**, the hydrazone analogue of **2**. It is worth noting that the
10
11 5 replacement of the sulphur atom of **2** with an oxygen in compound **7** implies a slight improvement
12
13 6 in the inhibitory activity against the PA-Nter enzyme, with the IC₅₀ changing from 37 to 24 μM.
14
15 7 This can be related to the improved ability of the ligand to interact with the metal cofactors, when a
16
17 8 harder donor atom is present. However, the activity of **7** in the cellular vRNP assay is lower than
18
19 9 that of the parent thiosemicarbazone **2**, thus suggesting that for the thiosemicarbazone compounds
20
21 10 inhibition of PA-Nter endonuclease is not the only mode of action. In influenza virus-infected cells,
22
23 11 in fact, the antiviral activity is higher for compound **4** than for **2**, and the other TSCs are inactive.
24
25 12 Note that, in cell culture (i.e. in the virus yield and vRNP reconstitution assay), **4** produces antiviral
26
27 13 activity at concentrations below 50 μM, while in the enzymatic assay its IC₅₀ value was 341 μM.
28
29 14 This suggests that the suppressive effect of **4** on influenza virus replication may not merely be
30
31 15 related to direct inhibition of the endonuclease enzyme, since the compound may also affect other
32
33 16 steps in the virus replicative cycle. These considerations are in line with our recent studies (20)
34
35 17 showing the complex biological properties of some molecules proposed as metal chelating
36
37 18 inhibitors of the influenza virus PA endonuclease.
38
39
40
41
42
43
44

45 **Conclusions**

46
47
48 21
49
50 22 We have started a project focused on synthesis and biological evaluation of chemical scaffolds that
51
52 23 are able to bind one or two metal ions in the PA-Nter active site and, in this way, can inhibit
53
54 24 influenza virus replication (20,22,40). From this perspective, salicylaldehyde thiosemicarbazones
55
56 25 seem promising, because of their well-known coordinating abilities and biological properties. In the
57
58 26 first evaluation reported here, positions 3, 4 and 5 of the phenyl ring were substituted with OH and
59
60

1
2
3 1 OCH₃ donor groups to derive a structure-activity relationship. Compounds **2** and **4** displayed
4
5 2 moderate activity in the PA Nter enzymatic assay and antiviral activity in both cell culture assays
6
7 3 used in this study. In particular, compound **2**, with two OH groups in position 2 and 3 on the phenyl
8
9 4 ring, is the most active and this is in line with the results recently reported by us with a 2,3-
10
11 5 dihydroxyphenyl amide inhibitor (22) and the literature regarding the use of natural polyphenols for
12
13 6 inhibiting influenza virus infection (52). Thiosemicarbazones **1-5** are effectively able to coordinate
14
15 7 magnesium(II) ion, as definitely proved by the structure of $\text{Mg}(\text{HL}^1)_2 \cdot 2\text{CH}_3\text{OH}$, but it seems
16
17 8 difficult to correlate their activity exclusively to this ability. For example, compound **5** is inactive,
18
19 9 while **4** is moderately active, but structural differences between them (5-methoxy group in **5** instead
20
21 10 of 5-OH group as in **4**) do not imply differences in chelating properties. The different activity could
22
23 11 depend on a different mechanism of action, but also on what Cohen sharply describes as “malleable
24
25 12 interaction” in metal coordination by metalloenzyme inhibitors (53), to describe the large number of
26
27 13 factors (donor atom identity, orientation, electrostatics, van der Waals interactions,...) that are
28
29 14 involved in the inhibition mechanism. Another point that deserves closer examination is the
30
31 15 difference between the data obtained for **2** and **4** by using different assays: in the enzyme assay, **2**
32
33 16 results more active than **4**, but the opposite was seen in virus-infected cells and the vRNP
34
35 17 reconstitution assay. Compound **4** probably acts by different antiviral mechanisms, not only metal
36
37 18 chelation. This underscores that characterization of the activity of a new compound is possible only
38
39 19 if different complementary assays are used.
40
41
42
43
44
45
46

47 21 Acknowledgments

48
49 22
50
51 23 The authors thank the “Centro Interfacoltà Misure *Giuseppe Casnati*” of the University of Parma
52
53 24 for facilities. L. Naesens and A. Stevaert acknowledge financial support from the Geconcerteerde
54
55 25 Onderzoeksacties – KU Leuven (GOA/15/019/TBA) and the technical assistance from Wim van
56
57 26 Dam, Leentje Persoons en Ria Van Berwaer.
58
59
60

1
2
3 **References**

- 4
5
6 [1] Deyde VM, Xu X, Bright RA, Shaw M, Smith CB, Zhang Y, Shu Y, Gubareva LV, Cox NJ,
7 Klimov AI (2007) *J. Infect. Dis.*, 196:249–257
8
9 [2] Moscona A (2009) *N. Engl. J. Med.*, 360:953–956
10
11 [3] Memoli MJ, Davis AS, Proudfoot K, Chertow DS, Hrabal RJ, Bristol T, Taubenberger JK
12 (2011) *J. Infect Dis.*, 203:348–357
13
14 [4] Van der Vries E, Schutten M, Fraaij P, Boucher C, Osterhaus A (2013) *Adv. Pharmacol.*
15 67:217-246
16
17 [5] Vanderlinden E, Naesens L (2014) *Med. Res. Rev.*, 34:301–339
18
19 [6] Honda A, Ishihama A (1997) *Biol. Chem.*, 378:483–488
20
21 [7] Honda A, Mizumoto K, Ishihama A (2002) *Proc. Natl. Acad. Sci. U.S.A.*, 99:13166–13171.
22
23 [8] Das K, Aramini JM, Ma LC, Krug RM, Arnold E (2010) *Nat. Struct. Mol. Biol.*, 17:530–538
24
25 [9] Dias A, Bouvier D, Crépin T, McCarthy AA, Hart DJ, Baudin F, Cusack S, Ruigrok RW
26 (2009) *Nature*, 458:914-918
27
28 [10] Yuan P, Bartlam M, Lou Z, Chen S, Zhou J, He X, Lv Z, Ge R, Li X, Deng T, Fodor E, Rao Z,
29 Liu Y (2009) *Nature*, 458:909-913
30
31 [11] Plotch SJ, Bouloy M, Ulmanen I, Krug RM (1981) *Cell*, 23:847–858
32
33 [12] Zhao C, Lou Z, Guo Y, Ma M, Chen Y, Liang S, Zhang L, Chen S, Li X, Liu Y, Bartlam M,
34 Rao Z (2009) *J. Virol.* 83:9024-9030
35
36 [13] DuBois RM, Slavish PJ, Baughman BM, Yun MK, Bao J, Webby RJ, Webb TR, White SW
37 (2012) *PLoS Pathog.*, 8:e1002830
38
39 [14] Kowalinski E, Zubieta C, Wolkerstorfer A, Szolar OH, Ruigrok RW, Cusack S (2012) *PLoS*
40 *Pathog.*, 8:e1002831
41
42 [15] Doan L, Handa B, Roberts NA, Klumpp K (1999) *Biochemistry*, 38:5612–5629
43
44
45
46
47
48
49
50
51
52
53
54
55
56
57
58
59
60

1
2
3
4
5
6
7
8
9
10
11
12
13
14
15
16
17
18
19
20
21
22
23
24
25
26
27
28
29
30
31
32
33
34
35
36
37
38
39
40
41
42
43
44
45
46
47
48
49
50
51
52
53
54
55
56
57
58
59
60

- [16] Xiao S, Klein ML, LeBard DN, Levine BG, Liang H, MacDermaid CM, Alfonso-Prieto M (2014) *J. Phys. Chem. B*, 118:873–889
- [17] Rogolino D, Carcelli M, Sechi M, Neamati N (2012) *Coord. Chem. Rev.*, 256:3063–3086
- [18] Tomassini JE, Selnick H, Davies ME, Armstrong ME, Baldwin J, Bourgeois M, Hastings J, Hazuda D, Lewis J, McClements W, Ponticello G, Radzilowski E, Smith G, Tebben A, Wolfe A (1994) *Antimicrob. Agents Chemother.*, 38:2827–2837
- [19] Hastings JC, Selnick H, Wolanski B, Tomassini JE (1996) *Antimicrob. Agents Chemother.* 40:1304–1307
- [20] Stevaert A, Nurra S, Pala N, Carcelli M, Rogolino D, Shepard C, Domaoal RA, Kim B, Alfonso-Prieto M, Marras SAE, Sechi M, Naesens L (2015) *Mol. Pharmacol.*, 87:323–337
- [21] Singh SB (1995) *Tetrahedron Lett.*, 36:2009–2012
- [22] Carcelli M, Rogolino D, Bacchi A, Rispoli G, Fisticaro E, Compari C, Sechi M, Stevaert A, Naesens L (2014) *Mol. Pharmaceutics*, 11:304–316
- [23] Parkes KEB, Ermert P, Fässler J, Ives J, Martin JA, Merrett JH, Obrecht D, Williams G, Klumpp K (2003) *J. Med. Chem.*, 46:1153–1164
- [24] Sagong HY, Parhi A, Bauman JD, Patel D, Vijayan RS, Das K, Arnold E, LaVoie EJ (2013) *ACS Med. Chem. Lett.*, 4:547–550
- [25] Knox JJ, Hotte SJ, Kollmannsberger C, Winqvist E, Fisher B, Eisenhauer EA (2007) *Invest. New Drugs*, 25:471–477
- [26] Kang IJ, Wang LW, Hsu TA, Yueh A, Lee CC, Lee YC, Lee CY, Chao YS, Shih SR, Chern JH (2011) *Bioorg. Med. Chem. Lett.*, 21:1948–1952
- [27] Quenelle DC, Keith KA, Kern ER (2006) *Antiv. Res.*, 71:24–30
- [28] Debebe Z, Ammosova T, Breuer D, Lovejoy DB, Kalinowski DS, Kumar K, Jerebtsova M, Ray P, Kashanchi F, Gordeuk VR, Richardson DR, Nekhai S (2011) *Mol. Pharmacol.*, 79:185–196

- 1
2
3 1 [29]Pelosi G, Bisceglie F, Bignami F, Ronzi P, Schiavone P, Re MC, Casoli C, Pilotti E (2010) J.
4
5 2 Med. Chem., 53:8765-8769
6
7 3 [30]Torti SV, Torti FM (2013) Nat. Rev. Cancer, 13:342-355
8
9 4 [31]Pelosi G (2010) Open Crystallography J., 3:16-28
10
11 5 [32]Sacconi L, (1954) Z. Anorg. Allg. Chem., 275:249-256
12
13 6 [33]Dolomanov OV, Bourhis LJ, Gildea RJ, Howard JAK, Puschmann H (2009) J. Appl. Cryst.,
14
15 7 42:339-341
16
17 8 [34]Burla MC, Caliandro R, Camalli M, Carrozzini B, Cascarano GL, De Caro L, Giacovazzo C,
18
19 9 Polidori G, Siliqi D, Spagna R (2007) J. Appl. Cryst., 40:609-613
20
21 10 [35]Sheldrick GM (2008) Acta Cryst., A64:112-122
22
23 11 [36]Nardelli M (1995) J. Appl. Cryst., 28:659
24
25 12 [37]Allen FH, Kennard O, Taylor R (1983) Acc. Chem. Res., 16:146-153
26
27 13 [38]Bruno IJ, Cole JC, Edgington PR, Kessler M, Macrae CF, McCabe P, Pearson J, Taylor R
28
29 14 (2002) Acta Crystallogr., B58:389-397
30
31 15 [39]Meneghesso S, Vanderlinden E, Stevaert A, McGuigan C, Balzarini J, Naesens L (2012)
32
33 16 Antiviral Res., 94:35-43
34
35 17 [40]Stevaert A, Dallochio R, Dessì R, Pala N, Rogolino D, Sechi M, Naesens L (2013) J. Virol.,
36
37 18 87:10524-10538
38
39 19 [41]Kim M, Kim SY, Lee HW, Shin JS, Kim P, Jung YS, Jeong HS, Hyun JK, Lee CK (2013)
40
41 20 Antiviral Res., 100:460-472
42
43 21 [42]Reed LJ, Muench H (1938) Am. J. Epidemiol., 27:493-497
44
45 22 [43]Vanderlinden E, Göktas F, Cesur Z, Froeyen M, Reed ML, Russell CJ, Cesur N, Naesens L
46
47 23 (2010) J. Virol., 84:4277-4288
48
49 24 [44]Gong Q, Menon L, Ilina T, Miller LG, Ahn J, Parniak MA, Ishima R (2011) Chem. Biol. Drug
50
51 25 Des., 77:39-47
52
53
54
55
56
57
58
59
60

1
2
3
4
5
6
7
8
9
10
11
12
13
14
15
16
17
18
19
20
21
22
23
24
25
26
27
28
29
30
31
32
33
34
35
36
37
38
39
40
41
42
43
44
45
46
47
48
49
50
51
52
53
54
55
56
57
58
59
60

- 1 [45] Enyedy ÉA, Zsigó É, Nagy NV, Kowol CR, Roller A, Keppler BK, Kiss T (2012) Eur. J. Inorg.
2 Chem., 4036-4047.
- 3 [46] Lobana TS, Kumari P, Hundal G, Butcher RJ (2010) Polyhedron, 29:1130–1136
- 4 [47] Chellan P, Stringer T, Shokar A, Dornbush PJ, Vazquez-Anaya G, Land KM, Chibale K, Smith
5 GS (2011) J. Inorg. Biochem., 105:1562–1568
- 6 [48] Ramachandran E, Kalaivani P, Prabhakaran R, Rath NP, Brinda S, Poornima P, Padma VV,
7 Natarajan K (2012) Metallomics, 4:218–227
- 8 [49] Kalaivani P, Prabhakaran R, Dallemer F, Poornima P, Vaishnavi E, Ramachandran E, Padma
9 VV, Renganathan R, Natarajan K (2012) Metallomics, 4:101–113
- 10 [50] West DX, Salberg MM, Bain GA, Liberta AE, Valdés-Martínez J, Hernández Ortega S (1996)
11 Transition Met. Chem., 21:206–212
- 12 [51] Sahadev RKS, Sindhwani SK (1992) Thermochemica Acta, 202:291-299
- 13 [52] Yang ZF, Bai LP, Huang WB, Li XZ, Zhao SS, Zhong NS, Jiang ZH (2014) Fitoterapia,
14 93:47–53
- 15 [53] Martin DP, Blachly PG, McCammon JA, Cohen SM (2014) J. Med. Chem. 57:7126–7135

1 **Table 1.** Crystal data and structure refinement for **2** and **Mg(HL¹)₂·2CH₃OH**.

	Mg(HL¹)₂·2MeOH	2
Empirical formula	C ₂₀ H ₂₈ MgN ₆ O ₆ S ₂	C ₁₀ H ₁₅ N ₃ O ₃ S
Formula weight	536.91	257.31
Temperature/K	293(2)	293
Crystal system	orthorhombic	monoclinic
Space group	P2nn	P2 ₁ /c
a/Å	7.878(1)	9.3259(6)
b/Å	10.639(2)	13.5879(9)
c/Å	31.921(5)	10.1652(6)
α/°	90	90
β/°	90	101.2117(9)
γ/°	90	90
Volume/Å ³	2675.4(7)	1263.5(1)
Z	4	4
ρ _{calc} /cm ³	1.333	1.353
μ/mm ⁻¹	0.267	0.257
F(000)	1128.0	544.0
Radiation	MoKα (λ = 0.71073)	MoKα (λ = 0.71073)
2θ range for data collection/°	2.552 to 44.106	4.452 to 63.216
Reflections collected	21724	19770
Independent reflections	3296 [R _{int} =0.0818, R _{sigma} = 0.0481]	4033 [R _{int} = 0.0263, R _{sigma} = 0.0184]
Data/restraints/parameters	3296/7/326	4033/0/174
Goodness-of-fit on F ²	1.073	1.031
Final R indexes [I>=2σ (I)]	R ₁ = 0.0702, wR ₂ = 0.1916	R ₁ = 0.0442, wR ₂ = 0.1267
Final R indexes [all data]	R ₁ = 0.0855, wR ₂ = 0.2057	R ₁ = 0.0492, wR ₂ = 0.1311
Largest ΔF max/min / e Å ⁻³	1.09/-0.38	0.81/-0.71
Flack parameter	0.43(7)	

2

3

Table 2. Inhibitory activity of compounds **1-7** in the enzymatic assay with influenza virus PA-Nter endonuclease, or cellular influenza virus assays based on virus yield or vRNP reconstitution.

Compound	Enzyme assay with PA-Nter ^a	Virus yield assay in influenza virus-infected MDCK cells ^b				vRNP reconstitution assay in HEK293T cells ^c	
		Antiviral activity		Cytotoxicity		Activity	Cytotoxicity
		IC ₅₀	EC ₉₉	EC ₉₀	MCC	CC ₅₀	EC ₅₀
(1)	>500	>200	>200	≥200	>200	>200	>200
(2)	37	≥87	≥56	≥100	≥138	63	>200
(3)	>500	>200	>200	>200	>200	>200	>200
(4)	341	48	34	≥100	146	22	>200
(5)	>500	>200	>200	≥200	>200	150	>200
(6)	>500	>100	>100	>200	>200	>100	>200
(7)	24	ND	ND	ND	ND	107	>200
DPBA ^d	5.5	ND	ND	ND	ND	ND	ND
Ribavirin	ND	13	8.5	≥200	>200	9.3	>200

^aRecombinant PA-Nter was incubated with the ssDNA plasmid substrate, a Mn²⁺-containing buffer and test compounds. Cleavage of the substrate was assessed after 2 hr incubation. The IC₅₀ represents the compound concentration (in μM) to obtain 50% inhibition of cleavage.

^bMDCK (Madin-Darby canine kidney) cells were infected with influenza A virus (strain A/PR/8/34) and incubated with the compounds during 24 hr. The virus yield in the supernatant was assessed by real-time qPCR. The EC₉₉ and EC₉₀ values represent the compound concentrations (in μM) producing a 2-log₁₀ or 1-log₁₀ reduction in virus titer, respectively. The cytotoxicity, assessed in uninfected MDCK cells, was expressed as the CC₅₀ value (50% cytotoxic concentration, determined with the MTS cell viability assay, in μM).

^cHEK293T (human embryonic kidney 293T) cells were cotransfected with the four vRNP-reconstituting plasmids and the luciferase reporter plasmid in the presence of the test compounds. The EC₅₀ value represents the compound concentration (in μM) producing 50% reduction in vRNP-driven firefly reporter signal, estimated at 24 h after transfection. The CC₅₀ (in μM), i.e. the 50% cytotoxic concentration, was determined in untransfected HEK293T cells by MTS cell viability assay.

^dDPBA, 2,4-dioxo-4-phenylbutanoic acid

ND, not determined.

Supporting Information

Investigation of the Salicylaldehyde Thiosemicarbazone Scaffold for Inhibition of Influenza Virus PA Endonuclease

Dominga Rogolino·Alessia Bacchi·Gabriele Rispoli·Mario Sechi·Annelies Stevaert·Lieve
Naesens·Mauro Carcelli

Dominga Rogolino·Alessia Bacchi·Gabriele Rispoli·Mauro Carcelli (✉)

Dipartimento di Chimica, Università di Parma, Parco Area delle Scienze 17/A, 43124 Parma, Italy

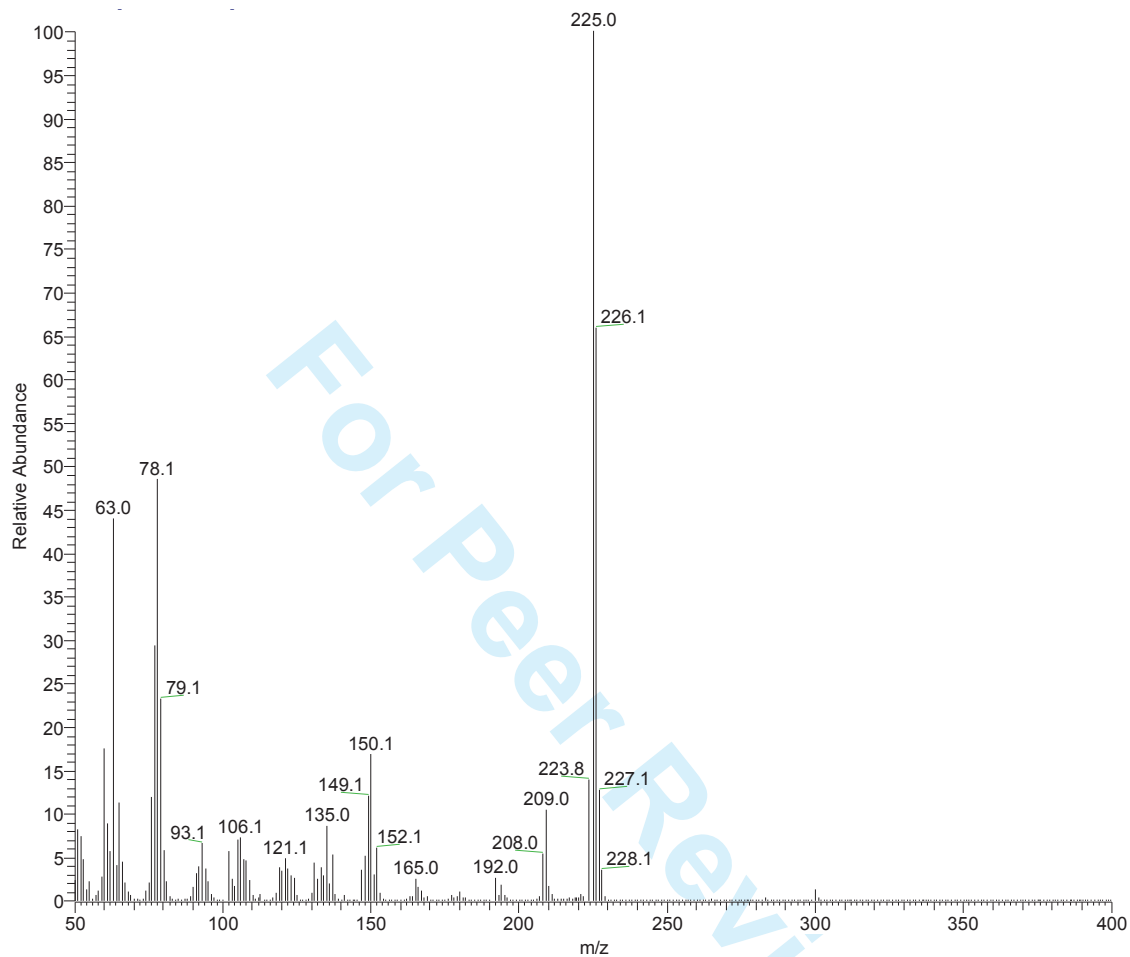
Email: mauro.carcelli@unipr.it

Mario Sechi

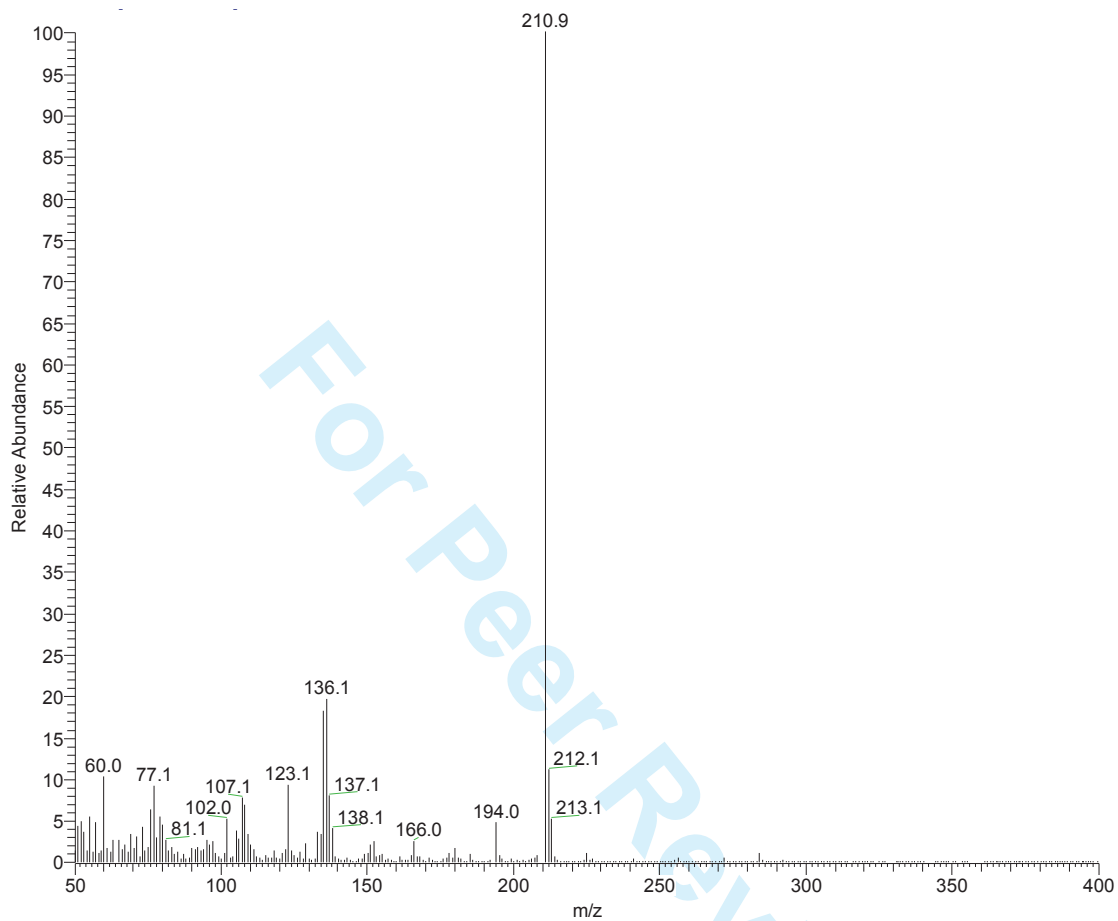
Dipartimento di Chimica e Farmacia, Università di Sassari, Via Vienna 2, 07100 Sassari, Italy

Annelies Stevaert·Lieve Naesens

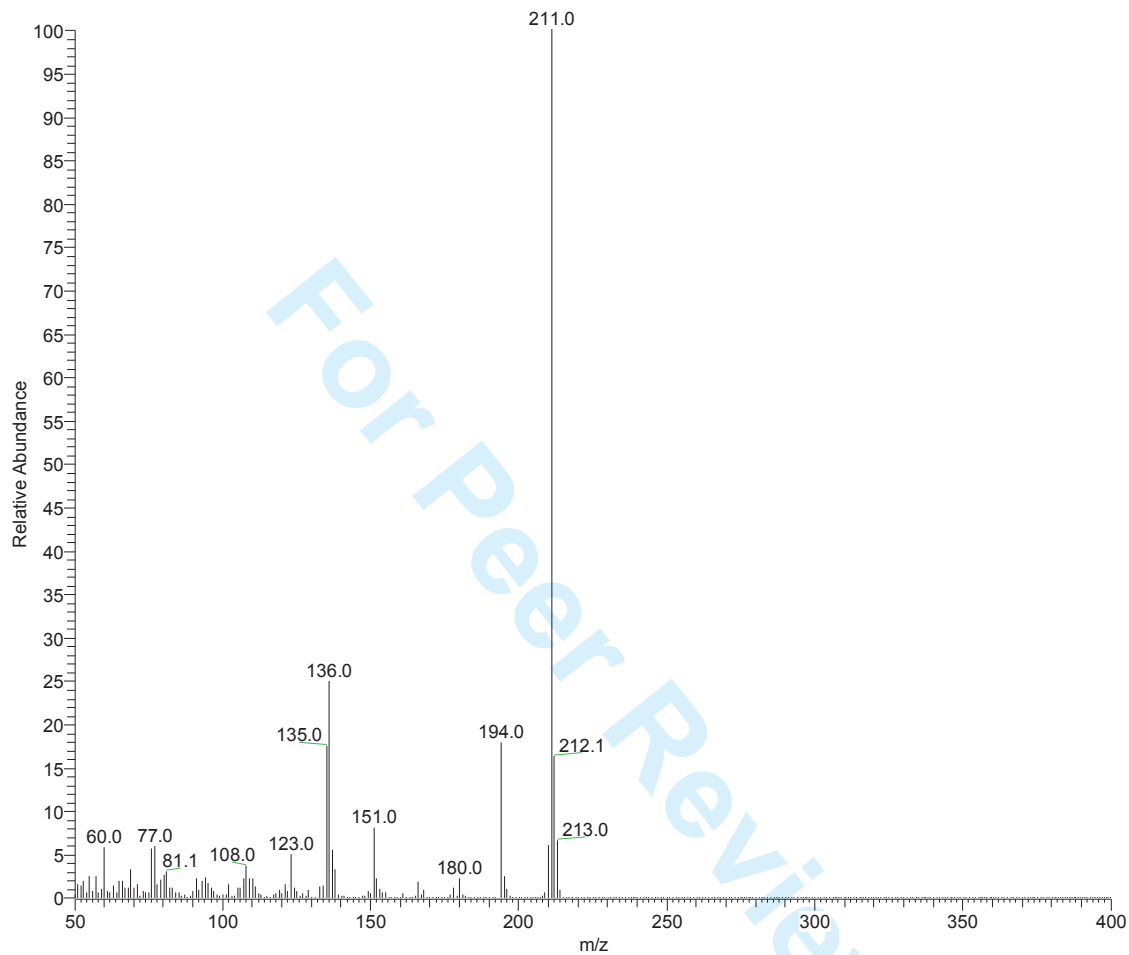
Rega Institute for Medical Research, KU Leuven, B-3000 Leuven, Belgium

Figure S1. Mass spectrum for compound **1** (EI, positive ions)

1
2
3 **Figure S2.** Mass spectrum for compound **2** (EI, positive ions)
4
5
6



1
2
3 **Figure S3.** Mass spectrum for compound **3** (EI, positive ions)
4
5
6
7
8



1
2
3 **Figure S4.** Mass spectrum for compound 4 (EI, positive ions)
4
5
6
7
8
9

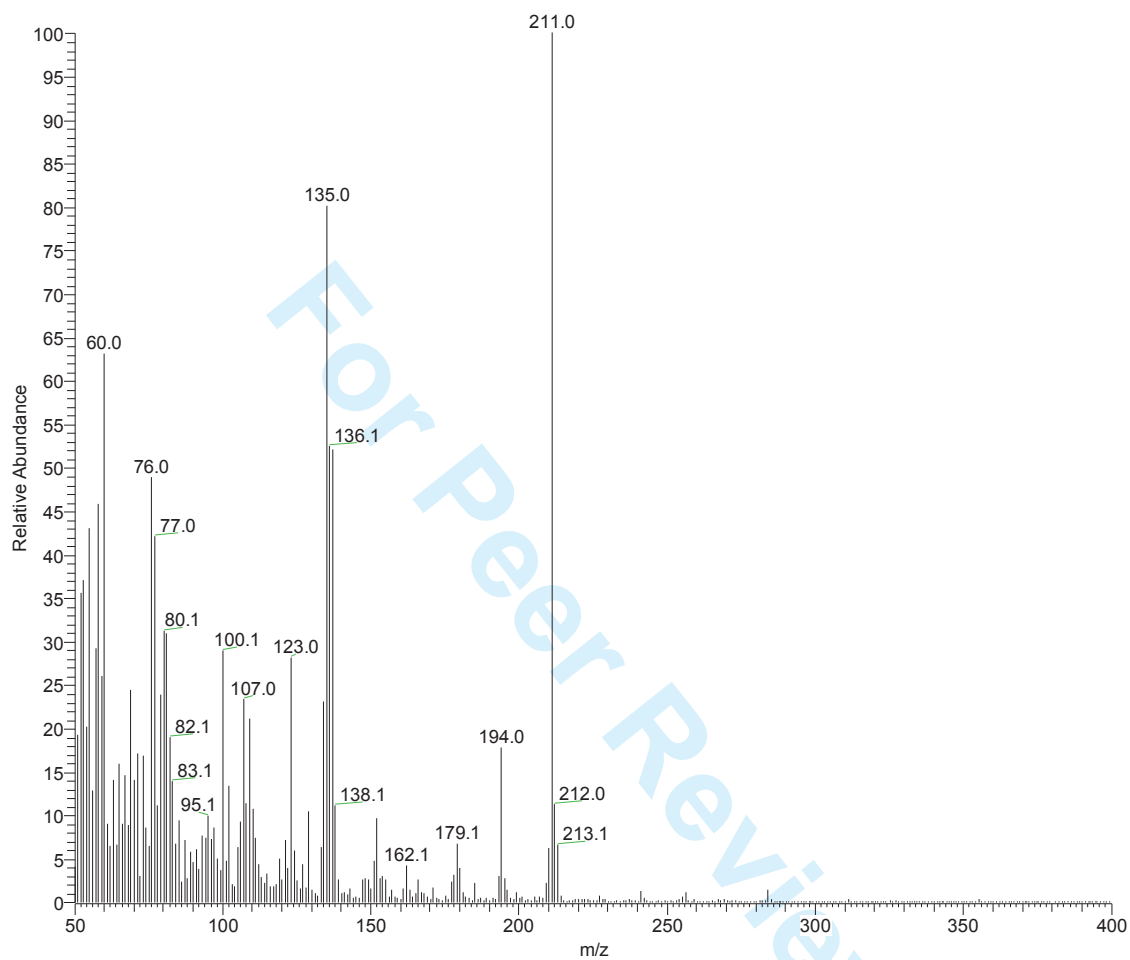
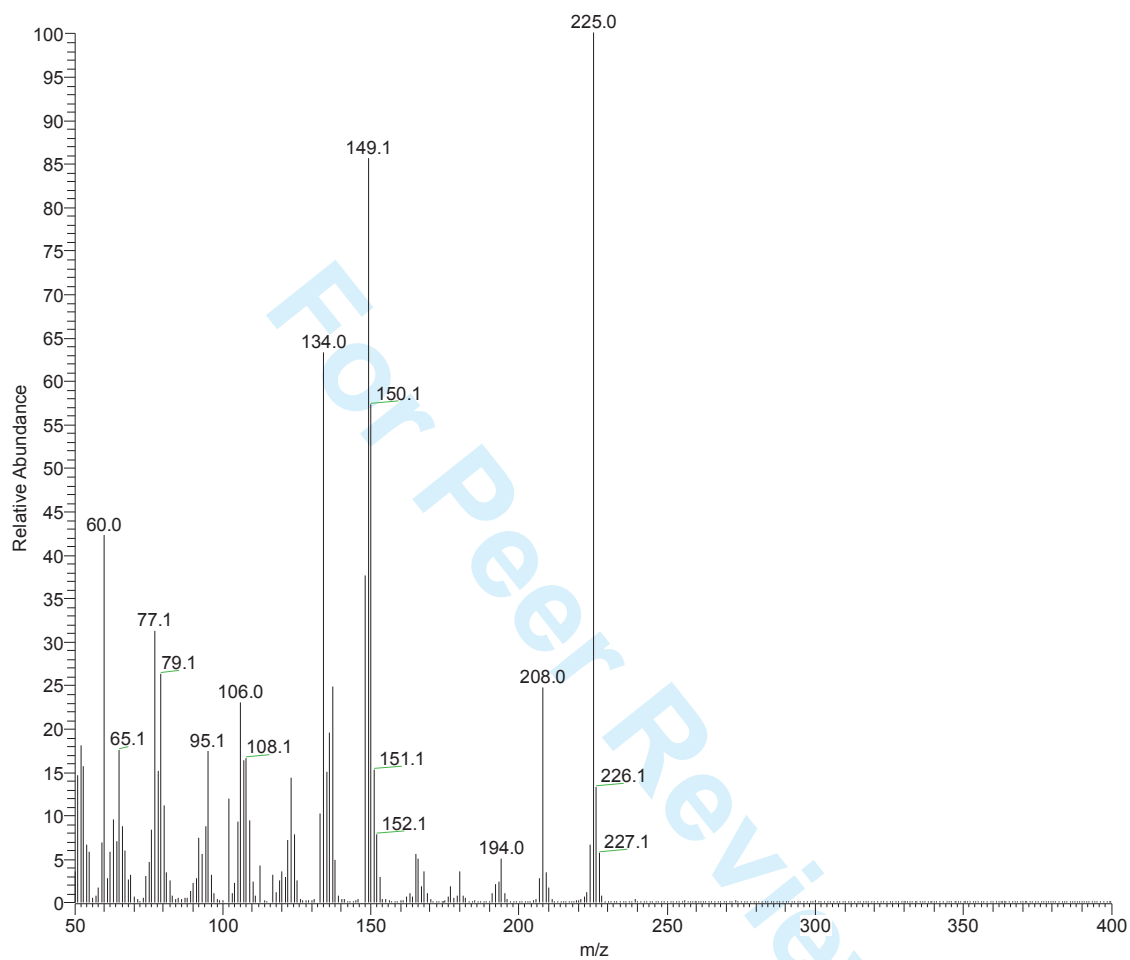
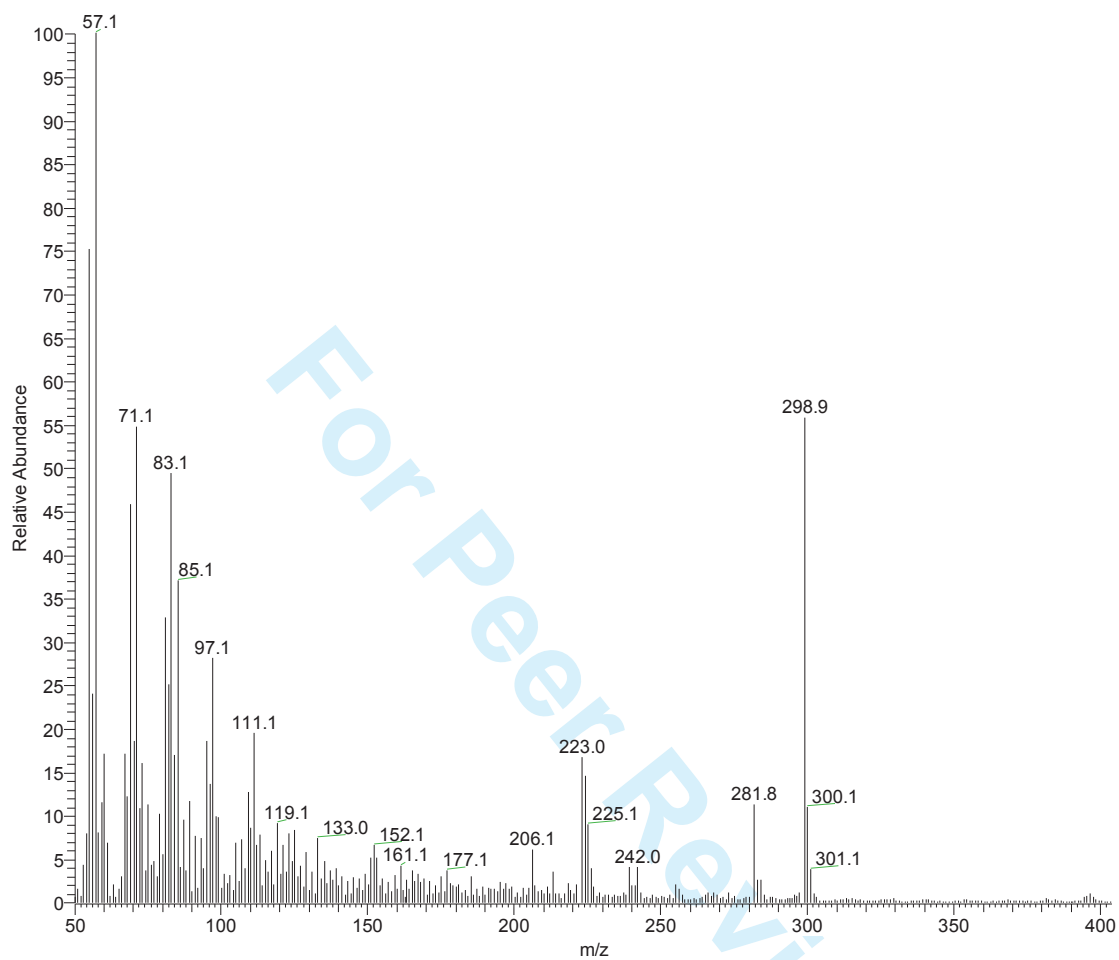
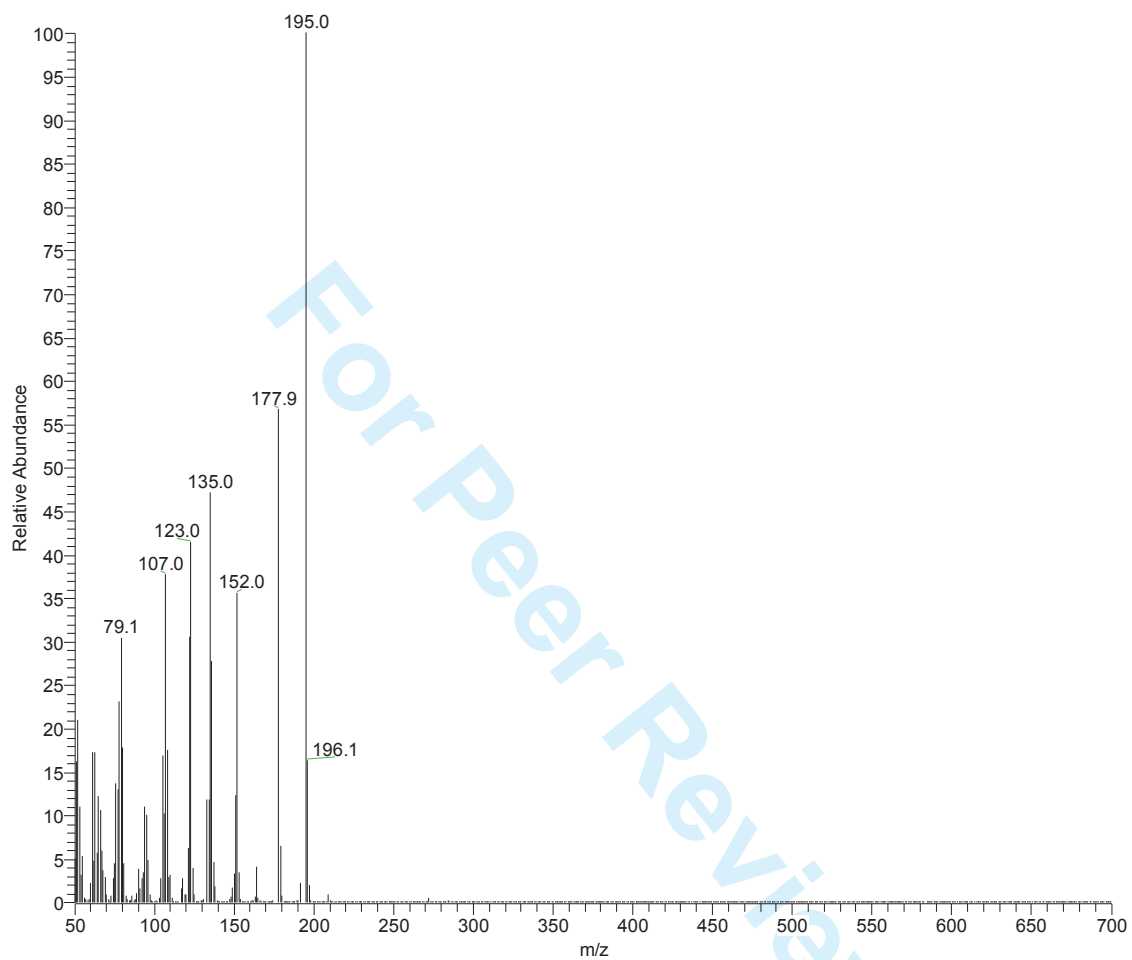


Figure S5. Mass spectrum for compound **5** (EI, positive ions)

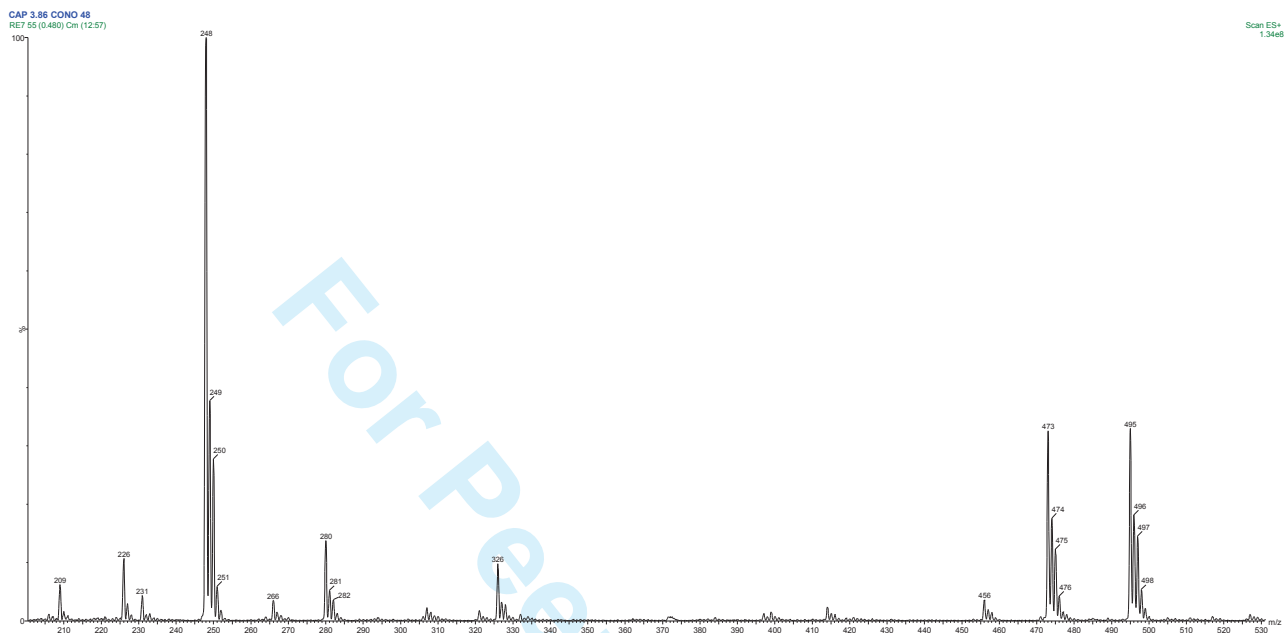
1
2
3 **Figure S6.** Mass spectrum for compound **6** (EI, positive ions)
4
5
6



1
2
3 **Figure S7.** Mass spectrum for compound 7 (EI, positive ions)
4
5
6
7
8
9



1
2
3 **Figure S8.** Mass spectrum for complex **8** (MS-ESI, positive ions)
4
5
6
7
8



1
2
3 **Figure S9.** Mass spectrum for complex **9** (MS-ESI, negative ions)
4
5
6
7
8
9

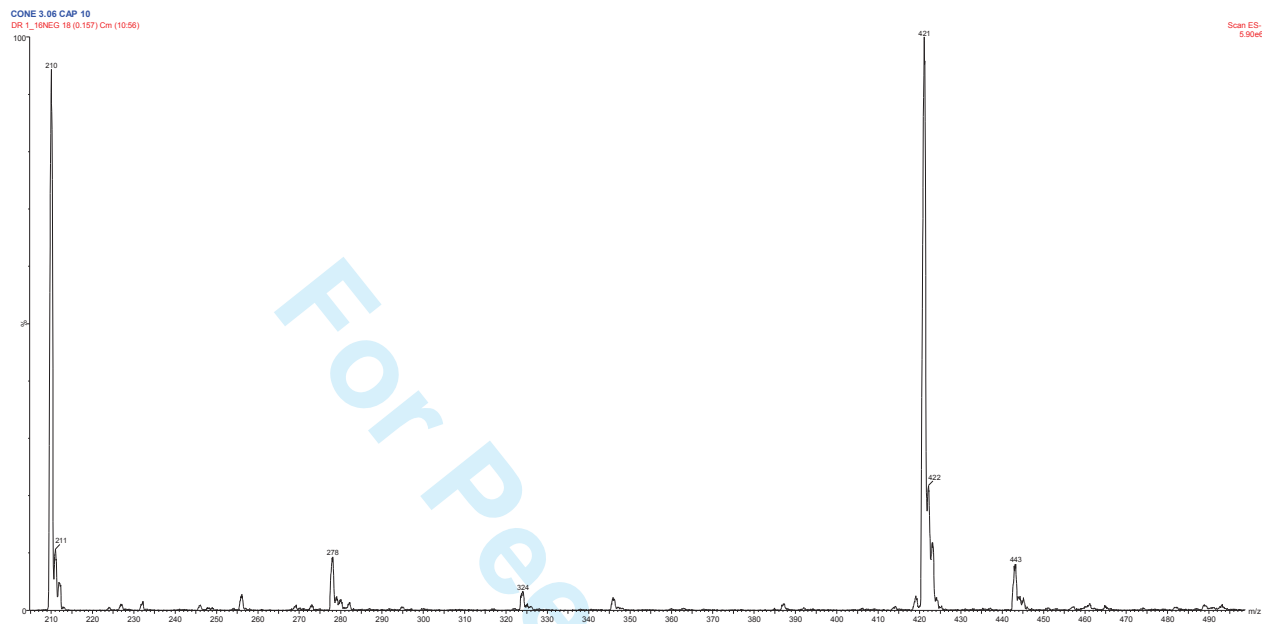


Figure S10. $^1\text{H-NMR}$ spectrum for complex **8** (MeOD, 400 MHz)